JOC The Journal of Organic Chemistry

pubs.acs.org/joc Article

Syntheses and Investigations of Conformationally Restricted, Linker-Free α-Amino Acid−BODIPYs via Boron Functionalization

Maodie Wang,[§] Guanyu Zhang,[§] Petia Bobadova-Parvanova, Kevin M. Smith, and M. Graça H. Vicente*

Cite This: J. Org. Chem. 2021, 86, 18030−18041 Read Online

ACCESS | Metrics & More | Article Recommendations | Supporting Information

ABSTRACT: A series of α-amino acid−BODIPY derivatives were synthesized using commercially available *N*-Boc-L-amino acids, via boron functionalization under mild conditions. The mono-linear, mono-spiro, and di-amino acid−BODIPY derivatives were obtained using an excess of basic (histidine, lysine, and arginine), acidic (aspartic acid), polar (tyrosine, serine), and nonpolar (methionine) amino acid residues, in yields that ranged from 37 to 66%. The conformationally restricted mono-spiro- and di-amino acid−BODIPYs display strong absorptions in the visible spectral region with high molar extinction coefficients and significantly enhanced fluorescence quantum yields compared with the parent BF_2−BODIPY. Cellular uptake and cytotoxicity studies using the human HEp2 cell line show that both the presence of an *N*,*O*-bidentate spiro-ring and basic amino acids (His and Arg) increase cytotoxicity and enhance cellular uptake. Among the series of BODIPYs tested, the spiro-Arg- and spiro-His-BODIPYs were found to be the most cytotoxic ($IC_{50} \sim 22\ \mu M$), while the spiro-His-BODIPY was the most efficiently internalized, localizing preferentially in the cell lysosomes, ER, and mitochondria.

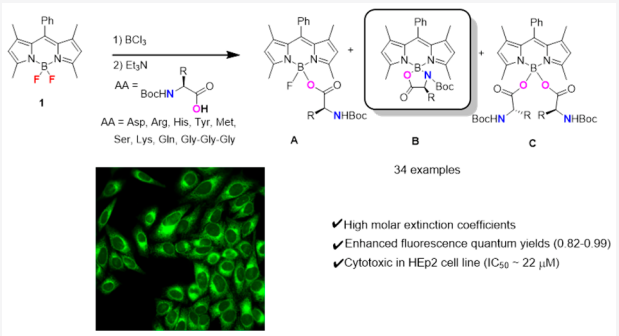

INTRODUCTION

Boron dipyrrin or boron dipyrromethene (BODIPY) dyes[1−6] are a class of boron-coordinated organic dyes that display a multitude of highly desirable properties for various applications, including good solubility in various solvents, large molar extinction coefficients, high fluorescence quantum yields, relatively sharp absorption and emission bands, low cytotoxicity, and structural tunability. With these extraordinary properties, BODIPY dyes have been widely applied in, for example, live-cell bioimaging,[7,8] photodynamic therapy,[9,10] fluorescent sensing,[11] dye-sensitized solar cells,[12] and viscosity detection.[13]

Several methodologies for the post-functionalization of BODIPYs have been developed over the past 2 decades.[12,14] The absorption and emission properties of BODIPY dyes can be fine-tuned from ca. 400[15,16] to 750 nm through functionalization reactions at the dipyrrin core.[14] In contrast, modifications at the boron center generally have little or no effect on the absorption and emission wavelengths, although the 3D structures of the boron-functionalized BODIPY molecules often change significantly upon the introduction of various groups at the boron atom. As a result, the fluorescence quantum yields, laser efficiencies,[17] redox behavior, aqueous solubility, aggregation behavior, and chemical stability[18−20] of BODIPYs can be conveniently fine-tuned for specific applications. Nucleophilic substitution of one or both fluorides at the boron position provides the possibility for application in positron emission tomography−optical dual imaging by replacing the nonradiative fluorine atom(s) by ^{18}F.[21] Other investigations of C-, O-, and N-BODIPYs[22−25] have led to enhanced materials for applications in energy-transfer cassettes, fluorescence imaging, and chiral recognition, among others. However, only a few reports have explored bidentate B-spiro-BODIPYs.[26−28]

Amino acid−fluorophore conjugates are important building blocks for the construction of bioactive fluorescent peptides and proteins. The synthesis of BODIPY−amino acid conjugates has been reported through C−H activation[29,30] and nucleophilic aromatic substitution reactions.[31] We have previously reported the synthesis of *N*,*O*-bidentate spiro-Gly-BODIPY derivatives by direct functionalization at the boron atom[32] and extended this methodology to the preparation of near-IR aza-BODIPY-Gln derivatives with potential application in photodynamic therapy.[33]

In the past few decades, the biological activities of boron-containing compounds have been investigated for their antifungal, antibacterial, antiviral, anti-inflammatory, and antiprotozoal activities.[34−37] Notably, tavaborole (Kerydin),

Received: September 22, 2021
Published: November 22, 2021

Scheme 1. Synthesis of α-Amino Acid–BODIPY Derivatives

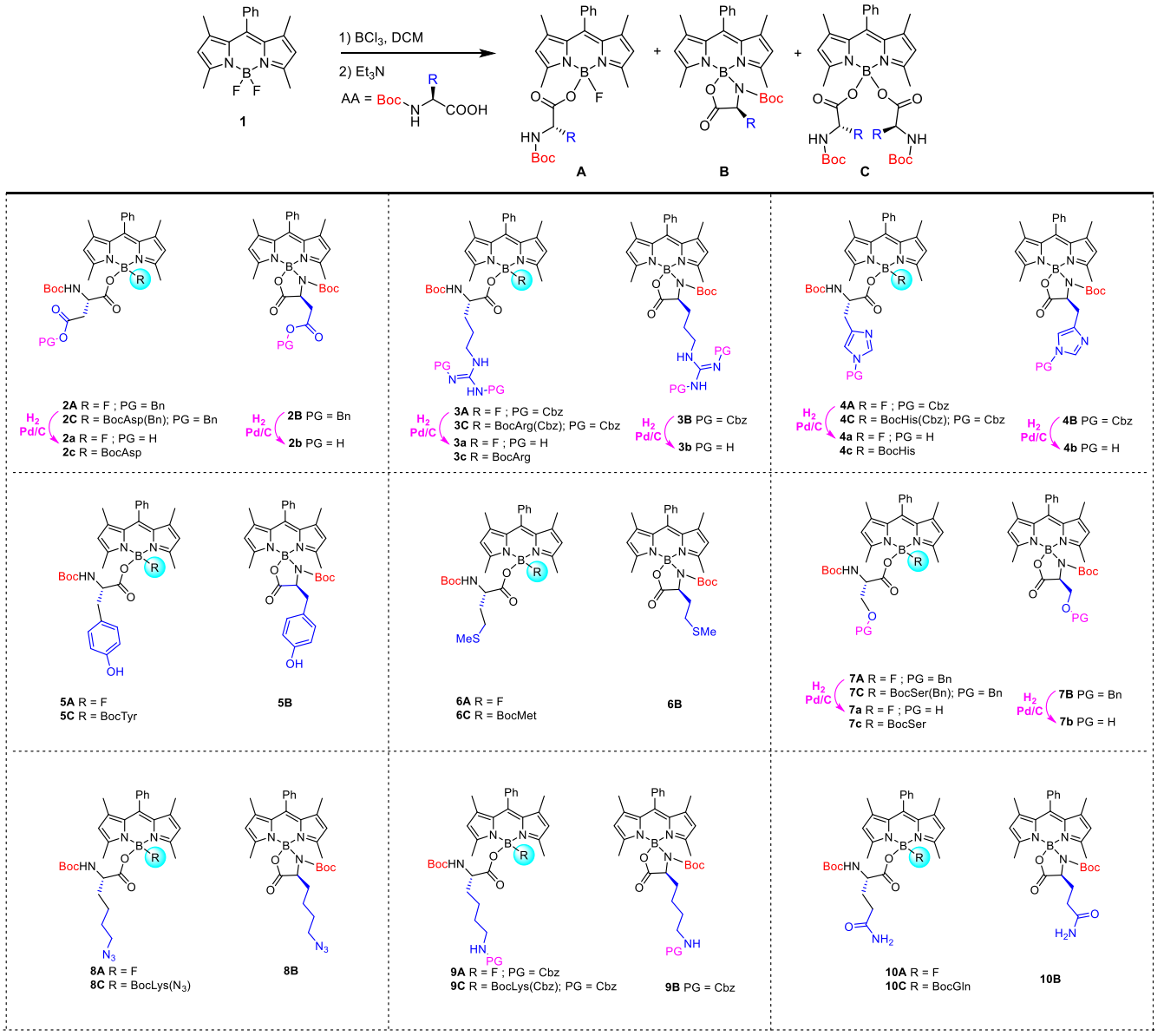

bortezomib (Velcade), and crisaborole (Eucrisa) have been studied for the treatment of onychomycosis, multiple myeloma, and atopic dermatitis, respectively.[38] Recently, in a study of NLRP3 inflammasome inhibitors, Freeman et al. reported that conformationally restricted analogues of a diarylboronic acid motif and an oxazaborine ring possessed enhanced anti-inflammatory activity.[39,40] Motivated by these studies, we set out to synthesize and investigate a series of conformationally restricted mono-spiro- and di-amino acid–BODIPY derivatives, bearing basic (histidine, lysine, and arginine), acidic (aspartic acid), polar (tyrosine, serine, and glutamine), and nonpolar (methionine) amino acid residues for potential therapeutic and/or imaging applications. In addition, a tripeptide $(Gly)_3$–BODIPY derivative was also prepared, showing that this methodology can be extended to the synthesis of linker-free BODIPY–peptide derivatives.

RESULTS AND DISCUSSION

Synthesis. BODIPY **1** was synthesized through a one-pot three-step method using 2,4-dimethylpyrrole and benzaldehyde as the starting materials following a reported procedure.[41] The reaction of BODIPY **1** with commercially available *N*-Boc L-amino acids, in the presence of boron trichloride, has wide substrate scope, as shown in Scheme 1. α-Amino acids bearing polar, nonpolar, cationic, and anionic side chains were used to produce the mono-(**A**), *N*,*O*-bidentate spiro-(**B**), and di-(**C**) α-amino acid BODIPY derivatives, in combined yields ranging from 37.3 to 65.9%. While BODIPYs **2** (Asp), **6** (Met), and **9** (Lys) were obtained in moderate yields (>60%), BODIPYs **4** (His) and **5** (Tyr) were isolated in lower yields (~40%), possibly due to the poor solubility of the amino acids in dichloromethane, as well as potential attack from the side chain on the boron center. A two-step one-pot reaction, previously reported using Gly[32] and Gln,[33] using two equivalents of boron trichloride and four equivalents of L-amino acid in dry dichloromethane at room temperature, was employed to

https://doi.org/10.1021/acs.joc.1c02328
J. Org. Chem. 2021, 86, 18030–18041

Scheme 2. Synthesis of $(Gly)_3$–BODIPY Conjugates

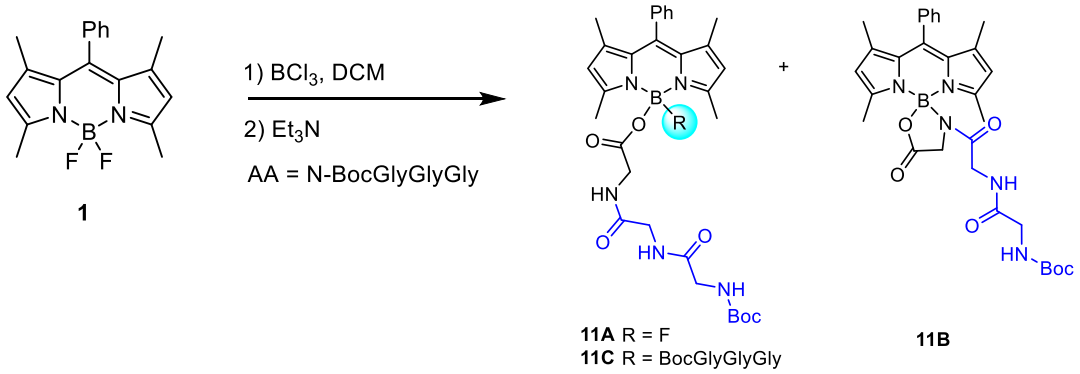

favor the formation of conformationally restricted products **B** and **C**. The *tert*-butyloxycarbonyl (Boc) electron-withdrawing group on the N-terminus of the amino acid is necessary for decreasing the charge on boron, therefore leading to stable N(sp^3) conjugates. Some amino acids bearing nucleophilic side chains also required the use of side chain protecting group(s) to avoid byproduct formation via a side chain attack on the boron atom. However, the widely used 9-fluorenylmethyloxycarbonyl (Fmoc) and trifluoroacetyl protecting groups require harsh conditions for deprotection,[42] which could also remove the *N*-Boc group and/or cause BODIPY degradation.[20] Therefore, the carboxylbenzyl (Cbz) or benzyl (Bn) groups were employed to protect the amino acids bearing nucleophilic side chains. The advantages of these two protecting groups are as follows: (1) the Cbz and Bn deprotection can be achieved under mild, neutral conditions in quantitative yields; (2) this strategy eliminates the formation of byproducts during the linker-free conjugation reaction; (3) the generated toluene product from Cbz or Bn deprotection is easily removed via vacuum evaporation; (4) Cbz or Bn protection can be applied to a variety of *O*,*N*-nucleophilic side chains; and (5) deprotection of the Cbz or Bn group does not affect the Boc group on the nitrogen adjacent to boron. Catalytic hydrogenation was performed to deprotect the Cbz or Bn side group(s) of the BODIPY derivatives (Scheme 1). The disappearance of the benzyl group (2H at ca. 5.0 ppm and 5H at ca. 7.5 ppm in $CDCl_3$) could be clearly seen by ^{1}H NMR, as shown in the Supporting Information. This methodology was successfully applied to the Asp-, Arg-, His-, and Ser-BODIPY conjugates, producing the corresponding **a**–**c** analogues. However, in the case of the Lys-BODIPY derivatives **9A**–**C**, upon the removal of the Cbz protecting group, the products decomposed within a few hours at room temperature, likely due to a nucleophilic attack of the amine upon the boron atom. The Arg-BODIPY was also observed to slowly decompose within 24 h; however, the His-BODIPY and all other derivatives bearing acidic, polar, and nonpolar amino acid side chains are stable in both solution and solid forms for at least 1 week at room temperature.

Presumably, the reaction of BODIPY **1** in the presence of boron trichloride proceeds via either the formation of a boronium cation intermediate,[41] followed by the nucleophilic attack of the amino acid carboxylate group on boron to produce product **A**, or via the in situ formation of a Cl_2-BODIPY intermediate[43−45] leading to products **B** and **C**.

The above methodology was extended to the synthesis of BODIPY derivative **8** bearing an azide-functionalized lysine residue suitable for further conjugation with alkyne-containing compounds via click chemistry. In addition, the tripeptide, *N*-Boc-GlyGlyGly was also prepared using this methodology, as shown in Scheme 2, producing *N*,*O*-bidentate $(Gly)_3$-BODIPY **11B** as the major product in 26.0% yield, followed by **11C** in 19.5% yield.

The structures of all α-amino acid-BODIPY conjugates were confirmed by ^{1}H, ^{13}C, ^{11}B-NMR, and high-resolution mass spectroscopy (HRMS) (see the Supporting Information). In all cases, the 9H in the Boc protecting groups can be seen at 1.4 ppm in the ^{1}H NMR spectra in the $CDCl_3$ solvent. The characteristic methyl protons at the 3,5-positions of the BODIPYs appear at ca. 2.2 ppm, while the protons at the 1,7-positions are shifted upfield to 1.3 ppm due to the shielding effect of the 8-phenyl ring. In the ^{1}H NMR, the protons at the α-carbon of the amino acid moiety are in the range of 4.5−5.0 ppm in $CDCl_3$, while the protons at the β-carbons are in the range of 3.0−4.0 ppm, depending on the side chain. Interestingly, the three products, **A**/**a**, **B**/**b**, and **C**/**c**, could be easily distinguished by ^{11}B-NMR as the spiro-(**B**/**b**) BODIPYs show one singlet at ∼1.9 ppm, while the mono-(**A**/**a**) BODIPYs show a doublet centered at ∼0.4 ppm and the di-(**C**/**c**) amino acid–BODIPYs show a singlet at ∼0.0 ppm.

Computational Studies. Our previous computational and NMR studies[32] showed that the spiro-Gly-BODIPY derivatives exist as two conformers (up and down) at room temperature, depending on the orientation of the Boc group with respect to the meso-phenyl, with the up-conformer being slightly more stable (ΔG < 3 kcal/mol). A similar trend is observed in the current series of amino acid-BODIPY derivatives. All the calculated data shown in Table S1 of the Supporting Information are for the up-conformers of the respective *N*,*O*-bidentate BODIPYs **B**. The mono-(**A**) and di-(**C**) amino acid–BODIPYs also exist in the form of two conformers with small energy differences (ΔG < 5 kcal/mol). All data discussed below refer to the more stable conformers.

Analysis of the calculated relative Gibbs energies of BODIPYs **2a**–**7a**, **2b**–**7b**, and **2c**–**7c** in dichloromethane demonstrates that the mono-substituted **a** is the most stable of the three forms, while the conformationally restricted spiro-compound **b** and the di-substituted **c** have similar Gibbs energies (see Table S1). The effect of the side chain is small and the energy differences range between 14 and 19 kcal/mol. However, experimentally BODIPYs bearing amino acids with strongly basic side chains, such as Arg and Lys, slowly decomposed in solution over a 24 h period, while all others, including His-BODIPY, were stable in solutions for over 1 week at room temperature. These results are consistent with previous observations of BODIPY instability under strongly

https://doi.org/10.1021/acs.joc.1c02328
J. Org. Chem. 2021, 86, 18030−18041

basic conditions, such as in the presence of ^{t}BuOK[46] or NH_4OH.[18] The lower stability of the di-substituted BODIPYs **c** compared with the mono-derivatives **a** is mostly due to entropy effects. On the other hand, the lower stability of the *N,O*-bidentate BODIPYs **b** is probably due to their relatively weaker B−N(Boc) bond compared with the B−O and B−F bonds. The B−N(Boc) bonds range between 1.541 and 1.547 Å with **3b** having the longest bond of the series (see Table S1). The B−N and B−O bond lengths are similar in all the investigated *N,O*-bidentate spiro-BODIPYs and do not change significantly when different amino acids are introduced. However, for all compounds in the series, the B−N(dipyrrin) bonds in the spiro-BODIPYs **b** are consistently 0.01−0.02 Å longer than the ones in the mono **a** and di-substituted **c** BODIPYs. Our previous studies on the stability of BODIPYs[16] suggest that the spiro-conjugates will therefore be slightly less stable than the di-substituted compounds. Furthermore, our calculations show that the *N,O*-bidentate **b** compounds are consistently more polar than the mono **a** and di-substituted **c** analogues throughout the entire series, with **2b** spiro-Asp being the most polar of all (see Table S1). The higher polarity of the *N,O*-bidentate spiro-compounds explains their observed higher solubility in polar solvents.

Spectroscopic Properties. The spectroscopic properties of the selected conformationally restricted BODIPYs **2b,c**, **3b,c**, **4b,c**, **5B,C**, **6B,C**, and **7b,c** were measured and calculated in acetonitrile. The experimental results are shown in Table 1,

Table 1. Spectroscopic Properties of α-Amino Acid−BODIPYs in Acetonitrile at Room Temperature[a]

BDP	λ_{abs} (nm)	log ε (M^{-1} cm^{-1})	λ_{em} (nm)	Φ_f[b]	Stokes' shift (nm)
1	498	4.92	509	0.61	11
2b	503	4.56	512	0.99	9
2c	503	4.80	515	0.98	12
3b	503	4.58	513	0.83	10
3c	503	4.32	513	0.90	10
4b	503	4.83	514	0.92	11
4c	503	4.76	514	0.89	11
5B	503	4.71	513	0.82	10
5C	503	4.78	513	0.93	10
6B	502	4.85	513	0.92	11
7b	503	4.43	512	0.95	9
7c	502	4.81	513	0.94	11

[a]According to our TD-DFT M06-2X/6-31+G(d,p) calculations in acetonitrile, the leading transition is HOMO → LUMO. All calculated data can be found in Table S2, Supporting information. [b]Fluorescein (0.91 in 0.1 M NaOH) was used as the standard.

and the calculated parameters are shown in the Supporting Information, Table S2. The bidentate spiro-(**B**) and the di-(**C**) amino acid-BODIPY derivatives have similar absorption and fluorescence profiles, with maximum absorption and emission bands centered at ca. 503 and 513 nm, respectively. These maximum absorption and emission wavelengths are slightly red-shifted (4−5 nm) compared with the parent BF_2-BODIPY **1**. This shift is in agreement with the performed TD-DFT calculations (Table S2). The predicted red shift is 3−5 nm and is due to the slightly smaller HOMO−LUMO gap for the α-amino acid−BODIPYs.

The similar absorption and emission profiles observed for this series of α-amino acid−BODIPYs are consistent with the calculated similar HOMO−LUMO energies and gaps, as shown in Figure 1 and the Supporting Information, Figure

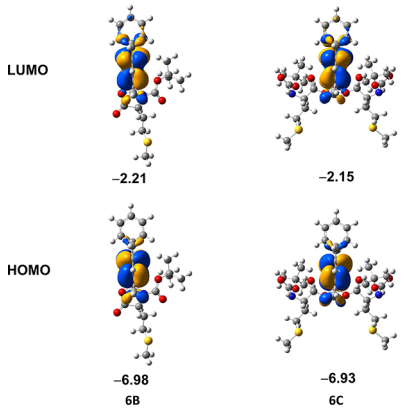

Figure 1. Frontier orbitals of BODIPYs **6B** and **6C**. Orbital energies in eV. The frontier orbitals of all conformers of all BODIPYs studied are given the Supporting Information (Figure S103).

S103. Figure 1 represents the frontier orbitals for the *N,O*-bidentate spiro and di-substituted BODIPYs **6B** and **6C**. Both HOMO and LUMO are localized on the BODIPY core with no significant contribution from the amino acid nor the Boc protecting group. This is also consistent with our previous findings[32] and is observed for all other α-amino acid−BODIPYs in the series. The performed TD-DFT calculations show that HOMO → LUMO is the leading transition for all BODIPYs studied. Given the fact that the forms and energies of these two orbitals are essentially independent of the amino acid, it is not surprising that the maximum absorption and emission wavelengths are very similar among the entire series.

Remarkably, all newly synthesized α-amino acid−BODIPYs display higher fluorescence quantum yields (Φ ∼ 0.9) compared with the parent BF_2−BODIPY **1** (Φ = 0.61), making them promising candidates for fluorescence labeling of bioactive peptides. As also suggested by our previous findings,[32] this result is probably due to the increased rigidity around the boron center in these conformationally restricted BODIPYs, which minimizes vibrations in-and-out of the dipyrrin plane. Interestingly, the calculated oscillator strengths of all α-amino acid−BODIPYs are smaller than that of parent BF_2-BODIPY **1**. However, the increased rigidity around the boron center most likely reduces the nonradiative vibrational relaxation, resulting in increased quantum yields.

Cellular Properties. *Cytotoxicity.* The cytotoxicity of the selected conformationally restricted α-amino acid−BODIPY **2b,c**, **3b,c**, **4b,c**, **5B**, **6B**, and **7b** were evaluated in human carcinoma HEp2 cells exposed to the increasing concentrations of each BODIPY up to 200 μM; the results are shown in the Supporting Information, Figures S104 and S105 and summarized in Table 2. Among the series (Figure S105), the spiro-Arg **3b** and spiro-His **4b** are the most toxic BODIPYs with IC_{50} values of 22 and 23 μM, respectively. These results indicate that both a spiro-5-membered ring on boron (as often observed in boron-based therapeutics, such as spiro-borates), and the presence of basic amino acids, such as Arg and His, increase the cytotoxicity of the compound. Indeed, a 3−5-fold increase in cytotoxicity was observed for the spiro-BODIPYs in comparison with the corresponding di-amino acid derivatives (Figure S105), possibly due to the more rigid *N,O*-bidentate

https://doi.org/10.1021/acs.joc.1c02328
J. Org. Chem. 2021, 86, 18030−18041

Table 2. Cytotoxicity of BODIPYs 2b,c, 3b,c, 4b,c, 5B, 6B, and 7b in HEp2 Cells Using the Cell Titer Blue Assay

Compound	Cytotoxicity (μM)
2b	58
2c	>200
3b	22
3c	104
4b	23
4c	68
5B	>200
6B	>200
7b	142

spiro-ring structure. On the other hand, basic amino acids such as Arg and His are capable of interacting with negatively charged groups on cell membranes and proteins, likely enhancing their cellular uptake and cytotoxicity. Previous studies of histidine-containing peptides showed a 2−8-fold increase in cytotoxicity as the solution pH decreased from 7.4 to 5.5,[47] suggesting that His-based compounds can be useful therapeutics. All the other spiro-BODIPYs evaluated bearing acidic (Asp), polar (Tyr), and nonpolar side chains showed low cytotoxicity with calculated IC_{50} values >142 μM.

Cellular Uptake and Intracellular Localization. The time-dependent cellular uptake of the most cytotoxic basic α-amino acid BODIPYs **3b** and **4b** and of the parent BODIPY **1** at a nontoxic concentration of 10 μM were evaluated in human carcinoma HEp2 cells (Figure 2). The basic amino acids Arg and His are able to interact with phosphate groups on plasma membranes, which enhances their cellular uptake. BODIPY **4b** containing His showed the highest uptake, about 2-fold that of the parent BODIPY **1** at times >2 h. The lower uptake observed for the Arg-BODIPY **3b**, compared with **4b** at all the times investigated, might in part be a result of its relatively lower stability due to the greater basicity of the guanidinium group. Although at times <8 h, BODIPY **3b** showed a lower uptake than parent BODIPY **1**, the positively charged guanidinium group in **3b** favored its continuous uptake over time via interaction with the negatively charged plasma membrane, thus leading to an enhanced uptake at 24 h relative to BODIPY **1**.[48,49]

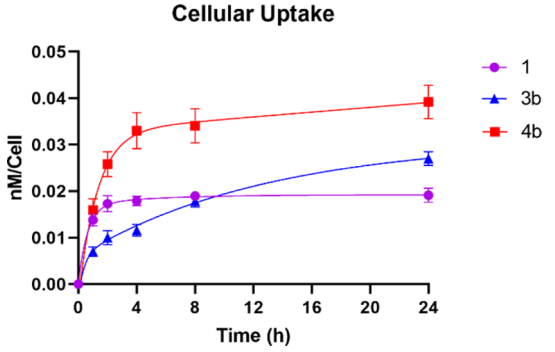

Figure 2. Time-dependent cellular uptake of BODIPYs **1** (purple), **3b** (blue), and **4b** (red) at 10 μM in human HEp2 cells.

The sub-cellular localization of BODIPYs **3b** (Figure 3) and **4b** (Figure 4) were also investigated by fluorescence microscopy upon the exposure of the HEp2 cells to 10 μM of each BODIPY for 6 h. Overlay experiments using the organelle-specific fluorescent probes LysoTracker deep red (lysosomes), MitoTracker deep red (mitochondria), ER Tracker blue/white (ER), and Hoechst 33342 (nuclei) were conducted to evaluate the preferential sites of BODIPY localization. The results obtained are shown in Figures 3 and 4. Both BODIPYs **3b** and **4b** are found to localize in the ER, mitochondria, and lysosomes. We have previously reported that BODIPY **1** accumulates preferentially in the ER, Golgi, and lysosomes.[19] Our results suggest that BODIPYs bearing positively charged amino acids (Arg, His) also localize in mitochondria, which might account for their observed higher cytotoxicity.

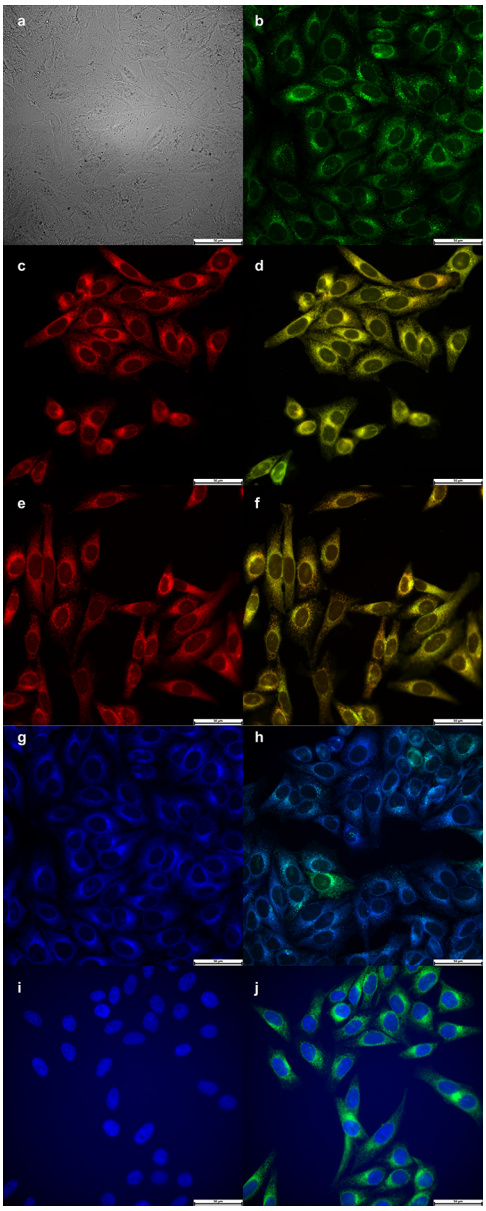

Figure 3. Sub-cellular localization of BODIPY **3b** in HEp2 cells at 10 μM after 6 h of incubation period. (a) Bright field; (b) fluorescence of BODIPY **3b**; (c) LysoTracker deep red; (e) MitoTracker deep red; (g) ER Tracker blue/white; (i) Hoechst 33342; and (d,f,h,j) overlays of tracers with BODIPY fluorescence. Scale bar: 50 μm.

CONCLUSIONS

A series of conformationally restricted α-amino acid−BODIPYs, bearing basic (His, Lys, and Arg), acidic (Asp),

https://doi.org/10.1021/acs.joc.1c02328
J. Org. Chem. 2021, 86, 18030−18041

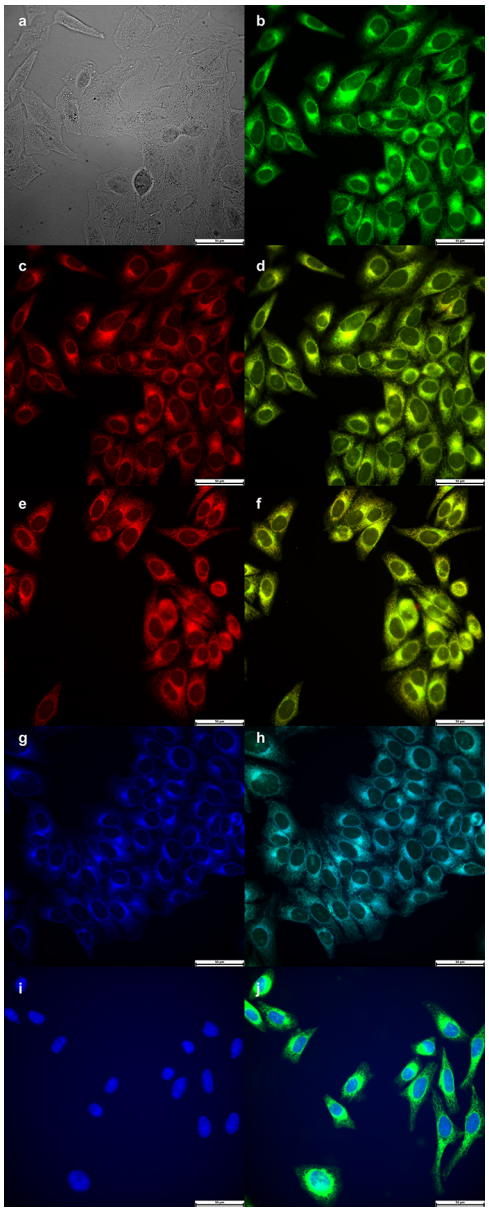

Figure 4. Sub-cellular localization of BODIPY **4b** in HEp2 cells at 10 μM after 6 h incubation period. (a) Bright field; (b) fluorescence of BODIPY **4b**; (c) LysoTracker deep red; (e) MitoTracker deep red; (g) ER Tracker blue/white; (i) Hoechst 33342; and (d,f,h,j) overlays of tracers with BODIPY fluorescence. Scale bar: 50 μm.

polar (Tyr, Ser), and nonpolar (Met) side chains, were synthesized in moderate yields from an in situ prepared BCl_2–BODIPY and *N*(Boc)-L-amino acids, at room temperature. The stability of these conformationally restricted BODIPYs depends on the amino acid binding mode and the basicity of its side chain, with the acidic, polar, and moderate basic (i.e., His) mono-linear amino acid–BODIPY derivatives being the most stable. The calculated relative Gibbs energies show that the *N*,*O*-bidentate spiro-BODIPYs are slightly less stable than the corresponding di-amino acid derivatives due to the weaker B–N(Boc) bond compared with the B–O bond.

The conformationally restricted amino acid–BODIPYs display similar absorption and emission properties, slightly red-shifted relative to the parent BF_2–BODIPY due to their slightly smaller HOMO–LUMO gap, and TD-DFT calculations suggest that HOMO → LUMO is the leading transition. Furthermore, all conformationally restricted amino acid–BODIPYs showed enhanced fluorescence quantum yields ($\Phi \sim 0.9$) compared with the parent BF_2–BODIPY ($\Phi = 0.61$) due to the increased rigidity around the boron center, which minimizes vibrations in-and-out of the dipyrrin plane.

Investigations in human HEp2 cells showed that the *N*,*O*-bidentate spiro-Arg and spiro-His are the most cytotoxic ($IC_{50} \sim 22$ μM), 3–5-fold more toxic than their corresponding di-amino acid BODIPY derivatives. The basic amino acid–BODIPYs are able to interact with negatively charged groups on plasma cell membranes showing an enhanced cellular uptake relative to the parent BF_2–BODIPY at 24 h. The preferential sites of intracellular localization for the most cytotoxic basic amino acid–BODIPYs were found to be the ER, mitochondria, and lysosomes, which might account for their observed higher cytotoxicity.

EXPERIMENTAL SECTION

General. Commercial grade chemical reagents were purchased from VWR or Sigma-Aldrich and used without further purification. Liquid column chromatography with silica gel (60 Å, 230–400 mesh) or preparative TLC plates (60 Å, 20 × 20 cm^2, 210–270 μm) were used for all the purifications. NMR spectra were collected using a Bruker AV-400 or AV-500 spectrometer at 300 K (operating at 400 or 500 MHz for ^1H, 126 MHz for ^{13}C NMR, and 128 MHz for ^{11}B NMR) in $CDCl_3$ (7.26 ppm for ^1H and 77.0 ppm for ^{13}C), CD_2Cl_2 (5.30 ppm for ^1H and 53.4 ppm for ^{13}C), CD_3OD (3.35 ppm for ^1H and 49.3 ppm for ^{13}C), and $BF_3{\cdot}OEt_2$ was set as a reference (0.00 ppm) for ^{11}B NMR. High-resolution mass spectra were collected at the LSU Department of Chemistry Mass Spectrometry Facility on an Agilent 6230-B ESI-TOF spectrometer in the positive mode. UV–vis absorption spectra were collected on a Varian Cary spectrophotometer. The fluorescence spectra were obtained using a PerkinElmer LS55 spectrophotometer. Emission spectra (λ_{ex} = 470 nm) were recorded in quartz cells. Relative fluorescence quantum yields (Φ_f) were calculated using Fluorescein (Φ_f = 0.91 in 0.1 M NaOH) as the standard for all compounds using the equation

$$\Phi_X = \Phi_{ST}\frac{\mathrm{Grad}_X}{\mathrm{Grad}_{ST}}\left(\frac{\eta_X}{\eta_{ST}}\right)^2$$

where Φ_X and Φ_{ST} are the quantum yields of the sample and standard, Grad_X and Grad_{ST} are the gradients from the plot of the integrated fluorescence intensity versus absorbance, and η represents the refractive index of the solvent. BODIPY **1** was prepared as previously reported in the literature.[41] Larger scale syntheses of **A**–**C** products have been previously reported.[33]

Computational Methods. The geometries of all compounds and complexes were optimized without symmetry constraints using the B3LYP/6-31+G(d,p) level.[50−52] The solvent effects were taken into account using the polarized continuum model.[53,54] The stationary points on the potential energy surface were confirmed with frequency calculations. The UV–vis absorption data were calculated using the TD-DFT method[55] All calculations were performed using the Gaussian 09 program package.[56]

Cell Culture. *Cytotoxicity.* All the cell culture media and reagents were purchased from VWR and fisher scientific. The human carcinoma HEp2 cells were purchased from ATCC and maintained in a MEM containing 5% FBS and 1% penicillin/streptomycin antibiotic. The cells were then sub-cultured and maintained twice weekly. Cell toxicity was evaluated using the CellTiter-Blue (Promega) assay.

The HEp2 cells were plated at 7500–10 000 cells per well in a Costar 96-well plate and allowed to grow for 24–48 h. BODIPY samples were dissolved in 100% DMSO to prepare 32 mM stock

https://doi.org/10.1021/acs.joc.1c02328
J. Org. Chem. 2021, 86, 18030–18041

solutions. Then, a 400 μM working solution was prepared for each sample. Through a 2-fold dilution procedure, HEp2 cells were exposed to concentrations of 0, 6.25, 12.5, 25, 50, 100, and 200 μM solutions and incubated for 24 h at 37 °C. The working solutions were then removed, and the cells were washed with 1 × PBS buffer triple times. The cells were exposed to the medium containing 20% CellTiterBlue and incubated for 4 h at 37 °C. The viability of the cells is measured by reading the fluorescence of the medium at 570/615 nm using a BMG FLUOstarOptima microplate reader. The fluorescence signal of the untreated cells in media only was normalized to 100%.

Cellular Uptake. Costar 96-well plates were prepared as described above. Each BODIPY solution (10 μM) was added to the cells and incubated for 0, 1, 2, 4, 8, and 24 h. At the end of the incubation period, the BODIPY solution was removed, and the cells were washed with 1 × PBS buffer triple times, followed by solubilizing the cells with 0.25% Triton X-100 in 1 × PBS buffer. The compound standard curve of each BODIPY was prepared by using BODIPY solutions with concentrations of 0, 0.31, 0.63, 1.25, 2.5, 5, and 10 μM in 1 × PBS buffer containing 0.25% X-100. The standard curve of the cell number was prepared using 10 000, 20 000, 40 000, 60 000, 80 000, and 100 000 cells per well and quantified by using a CyQuant Cell Proliferation Assay. The BODIPY concentration in cells at the end of each incubation period was determined using a BMG FLUOstar Optima microplate reader at the excitation wavelength and emission wavelength of each BODIPY. The time-dependent cellular uptake was evaluated as nM/cell.

Microscopy. The human HEp2 cells were incubated in a 35 mm tissue culture dish (CELLTREAT) and allowed to grow overnight. The cells were exposed to each compound at a concentration of 10 μM and incubated for 6 h (5% CO_2, 37 °C). The following organelle trackers (Invitrogen) were added to the cells: ER Tracker Blue/White (1 mM), Hoechst 33342 (16 mM), MitoTracker deep red (1 μM), and LysoSensor deep red (1 μM). The cells were incubated with each compound and trackers for half an hour, washed with PBS solution three times, and followed by fixing with 4% paraformaldehyde before imaging. A Leica DM6B upright microscope equipped with a 40 × water immersion objective, and DAPI, GFP, and Texas Red filter cubes (Chroma Technologies) were used to acquire the images.

Synthesis. *General Procedure for the Preparation of α-Amino Acid−BODIPY Derivatives.* BODIPY **1** (50 mg, 0.154 mmol) was dissolved in 5 mL of dry dichloromethane, followed by the addition of 2 equivalents of BCl_3 (1 M in toluene, 0.3 mL, 0.308 mmol). The reaction was stirred for 1 h at room temperature. Subsequently, a few drops of dry triethylamine were added to the reaction mixture. The N-protected amino acids (4 equivalents) were dissolved in a vial with dry dichloromethane and a few drops of dry triethylamine. The amino acid solutions were then added dropwise and stirred at room temperature for 1 h. The reaction mixture was then poured into a saturated $NaHCO_3$ solution and extracted with dichloromethane (10 mL × 3). The organic layers were combined and dried over anhydrous Na_2SO_4. The organic solvent was removed under reduced pressure, and the residue was purified by column chromatography on silica gel and recrystallized to afford the desired BODIPYs.

BODIPY **2** was synthesized using *N*-Boc-L-aspartic acid 4-benzyl ester (199.5 mg, 0.616 mmol) and purified by column chromatography using ethyl acetate/hexane (1:4). Compound **2A** was obtained as an orange solid (8.0 mg, 0.013 mmol, 8.4%): ^{1}H NMR (400 MHz, $CDCl_3$): δ 7.51−7.27 (m, 10H), 5.93 (d, *J* = 10.2 Hz, 2H), 5.51 (d, *J* = 7.5 Hz, 1H), 5.08 (q, *J* = 12.4 Hz, 2H), 4.45 (bs, 1H), 3.11 (dd, *J* = 16.4 Hz, 1H), 2.92 (dd, *J* = 16.8, 5.0 Hz, 1H), 2.48 (s, 3H), 2.36 (s, 3H), 1.41 (s, 9H), 1.38 (s, 6H). ^{13}C{^{1}H}NMR (126 MHz, $CDCl_3$): δ 170.9, 170.6, 170.5, 155.4, 155.1, 154.7, 143.4, 143.1, 142.2, 135.7, 135.0, 132.2, 129.2, 128.9, 128.9, 128.5, 128.3, 128.2, 127.9, 121.3, 79.5, 66.5, 51.0, 37.1, 28.3, 14.6, 14.5. ^{11}B NMR (128 MHz, $CDCl_3$): δ 0.40 (d, *J* = 23.2 Hz). HRMS (ESI-TOF) *m*/*z* [M + H]$^+$ calcd for $C_{35}H_{40}BFN_3O_6$, 628.2995; found, 628.3001. Compound **2B** was obtained as an orange solid (25.0 mg, 0.041 mmol, 26.6%): ^{1}H NMR (400 MHz, $CDCl_3$): δ 7.55−7.28 (m, 10H), 6.00 (d, *J* = 3.1 Hz, 2H), 5.28−5.18 (m, 2H), 4.97 (s, 1H), 3.19 (dd, *J* = 15.7, 4.8 Hz, 1H), 3.00 (dd, *J* = 15.8, 6.8 Hz, 1H), 2.34 (s, 3H), 2.30 (s, 3H), 1.39 (s, 3H), 1.37 (s, 3H), 1.19 (s, 9H). ^{13}C{^{1}H} NMR (126 MHz, $CDCl_3$): δ 175.8, 171.1, 156.0, 155.5, 154.6, 143.8, 143.5, 142.0, 136.1, 134.9, 133.2, 132.9, 129.6, 129.2, 129.1, 128.5, 128.4, 128.4, 128.2, 128.1, 127.4, 122.7, 122.7, 78.7, 66.8, 57.0, 36.5, 28.3, 16.4, 15.3, 14.7. ^{11}B NMR (128 MHz, CDCl3): δ 1.87 (s). HRMS (ESI-TOF) m/z [M + H]$^+$ calcd for $C_{35}H_{39}BN_3O_6$, 608.2933; found, 608.2945. Compound **2C** was obtained as an orange solid (41.0 mg, 0.044 mmol, 28.6%): ^{1}H NMR (400 MHz, $CDCl_3$): δ 7.50−7.28 (m, 15H), 5.89 (s, 2H), 5.50 (d, *J* = 7.4 Hz, 2H), 5.14−5.03 (m, 4H), 4.47 (s, 2H), 3.15−3.03 (m, 2H), 3.00−2.88 (m, 2H), 2.30 (s, 6H), 1.41 (s, 18H), 1.38 (s, 6H). ^{13}C{^{1}H} NMR (126 MHz, $CDCl_3$): δ 170.8, 170.6, 155.4, 153.9, 143.2, 135.6, 135.1, 132.6, 129.0, 128.9, 128.6, 128.3, 128.2, 121.5, 79.6, 66.6, 50.9, 36.9, 28.4, 14.7, 14.5. ^{11}B NMR (128 MHz, $CDCl_3$): δ 0.07 (s). HRMS (ESI-TOF) *m*/*z* [M + Na]$^+$ calcd for $C_{51}H_{59}BNaN_4O_{12}$, 953.4123; found, 953.4166.

BODIPY **3** was synthesized using $N_α$-Boc-$N_δ$,$N_ω$-di-carboxybenzyl-L-arginine (173.5 mg, 0.617 mmol) and purified by column chromatography using ethyl acetate/hexane (1:4) for elution. Compound **3A** was obtained as an orange solid (26.0 mg, 0.031 mmol, 20.0%): ^{1}H NMR (400 MHz, $CDCl_3$): δ 9.46 (s, 1H), 9.27 (s, 1H), 7.49−7.44 (m, 3H), 7.42−7.33 (m, 10H), 7.31−7.27 (m, 2H), 5.93 (s, 1H), 5.83 (s, 1H), 4.24 (d, *J* = 6.2 Hz, 1H), 4.05 (dd, *J* = 12.8, 7.5 Hz, 1H), 3.95 (d, *J* = 8.2 Hz, 1H), 2.44 (s, 3H), 2.40 (s, 3H), 1.92−1.82 (m, 1H), 1.58−1.46 (m, 2H), 1.39 (s, 9H), 1.37 (s, 3H), 1.35 (s, 3H). ^{13}C{^{1}H} NMR (126 MHz, $CDCl_3$): δ 172.0, 164.0, 160.6, 156.0, 155.3, 154.7, 143.3, 143.2, 142.3, 136.9, 135.0, 134.8, 132.3, 129.1, 128.9, 128.9, 128.8, 128.8, 128.4, 128.3, 128.2, 128.0, 127.9, 127.8, 121.3, 79.3, 68.9, 67.1, 54.2, 44.3, 31.6, 30.2, 29.7, 28.4, 24.9, 22.6, 14.6, 14.5, 14.4, 14.1. ^{11}B NMR (128 MHz, $CDCl_3$): δ 0.36 (d, *J* = 21.5 Hz). HRMS (ESI-TOF) *m*/*z* [M + H]$^+$ calcd for $C_{46}H_{53}BFN_6O_8$, 847.4004; found, 847.3984. Compound **3B** was obtained as an orange solid (26.0 mg, 0.032 mmol, 20.4%): ^{1}H NMR (400 MHz, $CDCl_3$): δ 9.49 (s, 1H), 9.30 (s, 1H), 7.54−7.46 (m, 3H), 7.45−7.38 (m, 6H), 7.38−7.29 (m, 4H), 7.29−7.26 (m, 1H), 7.25−7.20 (m, 1H), 5.94 (s, 2H), 5.26 (s, 2H), 5.15 (s, 2H), 4.15 (d, *J* = 8.1 Hz, 2H), 2.27 (s, 3H), 2.13 (s, 3H), 1.37 (s, 6H), 1.18 (s, 9H). ^{13}C{^{1}H} NMR (126 MHz, $CDCl_3$): δ 177.0, 164.0, 160.8, 156.1, 154.2, 143.7, 143.0, 141.8, 137.2, 135.0, 134.9, 133.1, 132.9, 129.5, 129.1, 129.0, 128.8, 128.6, 128.4, 128.4, 128.2, 127.9, 127.6, 127.5, 122.7, 122.5, 78.3, 68.8, 67.1, 60.0, 44.6, 31.6, 29.5, 28.3, 27.5, 22.6, 16.5, 15.0, 14.7, 14.6, 14.1. ^{11}B NMR (128 MHz, $CDCl_3$): δ 1.79(s). HRMS (ESI-TOF) *m*/*z* [M + H]$^+$ calcd for $C_{46}H_{52}BN_6O_8$, 827.3942; found, 827.3970. Compound **3C** was obtained as an orange solid (28 mg, 0.021 mmol, 13.2%): ^{1}H NMR (400 MHz, $CDCl_3$): δ 9.46 (s, 2H), 9.26 (s, 2H), 7.47−7.27 (m, 25H), 5.79 (s, 2H), 5.21 (s, 4H), 5.13 (s, 4H), 4.31−4.24 (m, 2H), 4.05 (dd, *J* = 13.3, 7.8 Hz, 2H), 3.95 (d, *J* = 5.4 Hz, 2H), 2.33 (d, *J* = 4.9 Hz, 2H), 2.30 (s, 6H), 1.89 (bs, 2H), 1.59−1.48 (m, 4H), 1.39 (s, 18H), 1.34 (s, 6H). ^{13}C{^{1}H} NMR (126 MHz, $CDCl_3$): δ 172.2, 164.0, 160.6, 155.9, 155.3, 153.5, 143.1, 137.0, 135.0, 134.7, 132.7, 128.9, 128.8, 128.8, 128.4, 128.3, 128.2, 128.0, 127.8, 121.4, 79.4, 68.9, 67.0, 54.2, 44.3, 31.6, 30.0, 28.4, 24.9, 22.6, 14.6, 14.1. ^{11}B NMR (128 MHz, $CDCl_3$): δ −0.06 (s). HRMS (ESI-TOF) *m*/*z* [M + H]$^+$ calcd for $C_{73}H_{86}BN_{10}O_{16}$, 1369.6328; found, 1369.6315.

BODIPY **4** was synthesized using *N*-Boc-L-histidine (240.2 mg, 0.617 mmol) and purified by column chromatography using ethyl acetate/hexane (1:1) for elution. Compound **4A** (trace, not isolated). Compound **4B** was obtained as an orange solid (27.0 mg, 0.040 mmol, 26.0%): ^{1}H NMR (400 MHz, $CDCl_3$): δ 8.13 (s, 1H), 7.57−7.34 (m, 10H), 7.24 (bs, 1H), 6.00 (d, *J* = 15.3 Hz, 2H), 5.39 (s, 2H), 4.63 (d, *J* = 7.5 Hz, 1H), 3.49 (d, *J* = 14.2 Hz, 1H), 3.18 (dd, *J* = 14.5, 9.4 Hz, 1H), 2.47 (s, 3H), 2.24 (s, 3H), 1.38 (s, 6H), 1.19 (s, 9H). ^{13}C{^{1}H} NMR (126 MHz, $CDCl_3$): δ 176.4, 156.1, 155.8, 148.8, 143.8, 143.2, 141.9, 141.5, 136.7, 135.0, 134.2, 133.1, 132.9, 129.5, 129.2, 129.1, 129.0, 128.8, 128.7, 128.4, 127.5, 122.7, 122.6, 114.4, 78.5, 69.6, 59.8, 31.6, 30.6, 28.3, 22.7, 16.7, 15.3, 14.7, 14.6, 14.1. ^{11}B NMR (128 MHz, $CDCl_3$): δ 1.81 (s). HRMS (ESI-TOF) *m*/*z* [M + H]$^+$ calcd for $C_{38}H_{41}BN_5O_6$, 674.3151; found, 674.3145. Compound **4C** was obtained as an orange solid (18.5 mg, 0.017 mmol, 11.3%):

https://doi.org/10.1021/acs.joc.1c02328
J. Org. Chem. 2021, 86, 18030−18041

^{1}H NMR (400 MHz, $CDCl_3$): δ 8.01 (s, 2H), 7.48−7.34 (m, 15H), 7.12 (s, 2H), 5.77 (s, 2H), 5.44 (d, J = 8.0 Hz, 2H), 5.37 (s, 4H), 4.53 (s, 2H), 3.20 (d, J = 5.0 Hz, 1H), 3.16 (d, J = 4.5 Hz, 1H), 3.05 (d, J = 6.0 Hz, 1H), 3.01 (d, J = 5.8 Hz, 1H), 2.24 (s, 6H), 1.36 (s, 18H), 1.34 (s, 6H). ^{13}C{^{1}H} NMR (126 MHz, $CDCl_3$): δ 171.6, 155.3, 148.5, 139.8, 136.6, 135.1, 134.1, 132.6, 129.2, 128.9, 128.7, 128.3, 121.2, 114.4, 79.3, 69.7, 53.6, 30.7, 28.3, 14.7, 14.6. ^{11}B NMR (128 MHz, $CDCl_3$): δ −0.01 (s). HRMS (ESI-TOF) m/z [M + Na]$^+$ calcd for $C_{57}H_{63}BN_8NaO_{12}$, 1085.4560; found, 1085.4526.

BODIPY **5** was synthesized using *N*-Boc-L-tyrosine (173.5 mg, 0.617 mmol) purified by column chromatography using ethyl acetate/hexanes (1:2) for elution. Compound **5A** was obtained as an orange solid (4.2 mg, 0.007 mmol, 4.6%): ^{1}H NMR (400 MHz, $CDCl_3$): δ 7.49−7.43 (m, 3H), 7.41−7.35 (m, 1H), 7.30−7.27 (m, 1H), 6.83 (d, J = 8.4 Hz, 2H), 6.56 (d, J = 8.0 Hz, 2H), 5.97 (s, 1H), 5.96 (s, 1H), 5.00 (d, J = 8.3 Hz, 1H), 4.47 (dd, J = 13.7, 5.7 Hz, 1H), 3.12 (dd, J = 13.9, 5.5 Hz, 1H), 2.90 (dd, J = 13.7, 6.0 Hz, 1H), 2.46 (s, 3H), 2.41 (s, 3H), 1.38 (s, 6H), 1.36 (s, 9H). ^{13}C{^{1}H} NMR (126 MHz, $CDCl_3$): δ 172.0, 155.3, 155.1, 154.2, 143.6, 143.2, 142.4, 134.9, 132.4, 130.4, 129.2, 128.9, 128.3, 127.8, 121.4, 121.2, 115.3, 79.5, 55.4, 37.5, 28.3, 21.1, 14.7, 14.5, 14.4, 14.2. ^{11}B NMR (128 MHz, $CDCl_3$): δ 0.45 (d, J = 18.3 Hz). HRMS (ESI-TOF) m/z [M + Na]$^+$ calcd for $C_{33}H_{37}BFNaN_3O_5$, 608.2708; found, 608.2703. Compound **5B** was obtained as an orange solid (22.6 mg, 0.040 mmol, 25.9%): ^{1}H NMR (400 MHz, $CDCl_3$): δ 7.59−7.39 (m, 7H), 6.82−6.75 (m, 2H), 6.03 (s, 1H), 5.97 (s, 1H), 4.41−4.33 (m, 1H), 3.42−3.36 (m, 1H), 3.16 (m, 1H), 2.48 (s, 3H), 2.19 (s, 3H), 1.39 (s, 3H), 1.38 (s, 3H), 1.23 (s, 9H). ^{13}C{^{1}H} NMR (126 MHz, $CDCl_3$): δ 177.0, 156.4, 155.9, 154.5, 143.8, 143.2, 141.8, 135.0, 133.0, 131.6, 131.0, 129.6, 129.2, 129.1, 128.4, 127.5, 122.7, 122.6, 115.3, 78.6, 53.8, 37.6, 28.4, 14.7, 14.6; ^{11}B NMR (128 MHz, $CDCl_3$): δ 1.82 (s). HRMS (ESI-TOF) m/z [M + H]$^+$ calcd for $C_{33}H_{36}BN_3O_5$, 566.2827; found, 566.2823. Compound **5C** was obtained as an orange solid (10.0 mg, 0.012 mmol, 7.7%): ^{1}H NMR (400 MHz, $CDCl_3$): δ 7.44 (bs, 3H), 7.39−7.33 (m, 2H), 6.91 (d, J = 7.5 Hz, 4H), 6.60 (d, J = 7.6 Hz, 4H), 5.92 (s, 2H), 5.01 (d, J = 8.0 Hz, 2H), 4.58−4.43 (m, 2H), 3.14−2.82 (m, 4H), 2.23 (s, 6H), 1.37 (bs, 24H). ^{13}C{^{1}H} NMR (126 MHz, $CDCl_3$): δ 172.2, 155.4, 155.1, 153.7, 143.4, 134.9, 132.6, 130.5, 129.0, 128.8, 128.2, 127.9, 121.4, 115.4, 79.8, 55.5, 37.6, 28.3, 14.7, 14.6; ^{11}B NMR (128 MHz, $CDCl_3$): δ −0.01 (s). HRMS (ESI-TOF) m/z [M + Na]$^+$ calcd for $C_{47}H_{55}BNaN_4O_{10}$, 869.3912; found, 869.3925.

BODIPY **6** was synthesized using *N*-Boc-L-methionine (153.8 mg, 0.617 mmol), purified by preparative TLC plates using ethyl acetate/dichloromethane/hexanes (1:1:6) for elution. Compound **6A** (trace product, not isolated). Compound **6B** was obtained as an orange solid (19.1 mg, 0.036 mmol, 23.2%): ^{1}H NMR (400 MHz, CD_2Cl_2): δ 7.51−7.47 (m, 3H), 7.31−7.27 (m, 1H), 7.24 (bs, 1H), 6.03 (s, 1H), 6.02 (s, 1H), 4.26 (dd, J = 8.6, 3.0 Hz, 1H), 3.01−2.94 (m, 1H), 2.92−2.84 (m, 1H), 2.36 (s, 3H), 2.21 (s, 3H), 2.15 (s, 3H), 1.38 (s, 3H), 1.37 (s, 4H), 1.16 (s, 9H). ^{13}C{^{1}H} NMR (126 MHz, $CDCl_3$): δ 176.9, 156.1, 155.9, 154.2, 143.8, 143.2, 141.8, 134.9, 133.0, 132.9, 129.5, 129.1, 129.0, 128.3, 127.4, 122.7, 122.5, 78.4, 59.2, 32.4, 31.6, 28.2, 16.6, 15.3, 15.1, 14.7, 14.6; ^{11}B NMR (128 MHz, $CDCl_3$): δ 1.83 (s). HRMS (ESI-TOF) m/z [M + H]$^+$ calcd for $C_{29}H_{37}BN_3O_4S$ 534.2598; found, 534.2623. Compound **6C** was obtained as an orange solid (49.2 mg, 0.063 mmol, 40.8%): ^{1}H NMR (500 MHz, $CDCl_3$): δ 7.50−7.43 (m, 3H), 7.41−7.33 (m, 2H), 5.94 (s, 2H), 5.15 (d, J = 7.6 Hz, 2H), 4.37 (d, J = 4.1 Hz, 2H), 2.57−2.51 (m, 2H), 2.41 (s, 6H), 2.28−2.18 (m, 2H), 2.09 (s, 6H), 1.93−1.84 (m, 2H), 1.42 (s, 18H), 1.39 (s, 6H). ^{13}C{^{1}H} NMR (126 MHz, $CDCl_3$): δ 171.8, 155.2, 153.3, 143.3, 142.7, 134.8, 132.6, 129.0, 128.9, 128.0, 121.4, 79.5, 53.7, 34.6, 32.8, 31.5, 29.0, 28.3, 25.2, 15.5, 14.8, 14.6, 14.0; ^{11}B NMR (128 MHz, $CDCl_3$): δ 0.03 (s). HRMS (ESI-TOF) m/z [M + Na]$^+$ $C_{39}H_{55}BNaN_4O_8S_2$, calcd for 805.3454; found, 805.3463.

BODIPY **7** was synthesized using *N*-Boc-*O*-benzyl-L-serine (182.2 mg, 0.617 mmol) and purified by preparative TLC plates using ethyl acetate/dichloromethane/hexanes (1:1:6) for elution. Compound **7A** was obtained as an orange solid (4.4 mg, 0.007 mmol, 4.8%): ^{1}H NMR (500 MHz, $CDCl_3$): δ 7.53−7.46 (m, 3H), 7.45−7.41 (m, 1H), 7.33−7.27 (m, 4H), 7.25−7.21 (m, 2H), 5.95 (s, 1H), 5.89 (s, 1H), 5.50 (d, J = 8.1 Hz, 1H), 4.54−4.46 (m, 2H), 4.42−4.34 (m, 1H), 4.05 (dd, J = 9.2, 2.3 Hz, 1H), 3.75 (dd, J = 9.2, 2.6 Hz, 1H), 2.45 (s, 3H), 2.42 (s, 3H), 1.44 (s, 9H), 1.41 (s, 3H), 1.40 (s, 3H). ^{13}C{^{1}H} NMR (126 MHz, $CDCl_3$): δ 170.2, 170.1, 155.4, 155.2, 154.6, 143.3, 143.0, 142.2, 138.0, 135.1, 132.3, 132.2, 129.2, 128.9, 128.3, 128.2, 127.9, 127.5, 127.4, 121.4, 121.3, 79.4, 73.1, 70.7, 55.0, 53.5, 28.4, 14.6, 14.5. ^{11}B NMR (128 MHz, $CDCl_3$): δ 0.41 (d, J = 24.3 Hz). HRMS (ESI-TOF) m/z [M + Na]$^+$ $C_{34}H_{39}BFNaN_3O_5$, calcd for 622.2865; found, 622.2860. Compound **7B** was obtained as an orange solid (27.0 mg, 0.047 mmol, 30.2%): ^{1}H NMR (400 MHz, $CDCl_3$): δ 7.49 (bs, 3H), 7.44−7.38 (m, 2H), 7.38−7.29 (m, 3H), 7.29−7.27 (m, 1H), 7.25−7.22 (m, 1H), 5.98 (s, 1H), 5.94 (s, 1H), 4.70 (s, 2H), 4.47 (s, 1H), 4.20−4.07 (m, 2H), 2.33 (s, 3H), 2.27 (s, 3H), 1.37 (s, 3H), 1.36 (s, 3H), 1.22 (s, 9H). ^{13}C{^{1}H} NMR (126 MHz, $CDCl_3$): δ 175.5, 157.2, 156.2, 153.9, 144.1, 142.9, 141.7, 138.4, 135.0, 133.1, 129.5, 129.2, 129.0, 128.5, 128.2, 127.8, 127.5, 127.4, 122.9, 122.5, 78.6, 73.2, 69.3, 61.5, 28.3, 16.4, 15.2, 14.8, 14.6; ^{11}B NMR (128 MHz, $CDCl_3$): δ 1.99 (s). HRMS (ESI-TOF) m/z [M + H]$^+$ calcd for $C_{34}H_{39}BN_3O_5$ 580.2983; found, 580.2987. Compound **7C** was obtained as an orange solid (31.0 mg, 0.036 mmol, 23.2%): ^{1}H NMR (400 MHz, $CDCl_3$): δ 7.51−7.39 (m, 5H), 7.33−7.27 (m, 5H), 7.24−7.17 (m, 5H), 5.83 (s, 2H), 5.45 (d, J = 7.9 Hz, 2H), 4.49 (q, J = 12.2 Hz, 4H), 4.37 (d, J = 6.9 Hz, 2H), 4.03 (d, J = 8.6 Hz, 2H), 3.74 (d, J = 8.4 Hz, 2H), 2.27 (s, 6H), 1.42 (s, 18H), 1.39 (s, 6H). ^{13}C{^{1}H} NMR (101 MHz, $CDCl_3$): δ 170.2, 155.4, 154.0, 143.0, 137.8, 135.2, 132.7, 129.0, 128.8, 128.3, 127.6, 127.5, 121.4, 79.4, 73.1, 70.5, 54.9, 28.4, 14.6, 14.5; ^{11}B NMR (128 MHz, $CDCl_3$): δ 0.04 (s). HRMS (ESI-TOF) m/z [M + Na]$^+$ calcd for $C_{49}H_{59}BN_4NaO_{10}$, 897.4225; found, 897.4235.

BODIPY **8** was synthesized using *N*-Boc-L-azidolysine (168.0 mg, 0.617 mmol) and purified by preparative TLC plates using ethyl acetate/dichloromethane/hexanes (1:1:6) for elution. Compound **8A** was obtained as an orange solid (12.0 mg, 0.021 mmol, 13.5%): ^{1}H NMR (400 MHz, $CDCl_3$): δ 7.52−7.45 (m, 3H), 7.42−7.38 (m, 1H), 7.30−7.26 (m, 1H), 5.96 (s, 2H), 5.19 (d, J = 7.5 Hz, 1H), 4.27 (dd, J = 11.8, 6.7 Hz, 1H), 3.23 (d, J = 7.2 Hz, 2H), 2.47 (s, 6H), 2.00−1.86 (m, 1H), 1.75−1.64 (m, 1H), 1.60−1.51 (m, 2H), 1.41 (s, 9H), 1.39 (s, 6H), 1.23−1.16 (m, 1H). ^{13}C{^{1}H} NMR (126 MHz, $CDCl_3$): δ 172.1, 155.3, 154.9, 154.2, 143.5, 143.3, 142.4, 134.9, 132.3, 129.2, 129.0, 128.2, 127.9, 121.4, 121.2, 79.3, 54.1, 51.4, 32.6, 28.7, 28.4, 22.3, 14.7, 14.7, 14.6, 14.6, 14.5, 14.5; ^{11}B NMR (128 MHz, $CDCl_3$): δ 0.39 (d, J = 24.4 Hz). HRMS (ESI-TOF) m/z [M + H]$^+$ calcd for $C_{30}H_{39}BFN_6O_4$, 577.3110; found, 577.3114. Compound **8B** was obtained as an orange solid (19.2 mg, 0.035 mmol, 22.4%): ^{1}H NMR (400 MHz, $CDCl_3$): δ 7.48 (bs, 3H), 7.25−7.19 (m, 2H), 5.98 (d, J = 7.0 Hz, 2H), 4.12 (d, J = 8.6 Hz, 1H), 3.29 (t, J = 18.5, 11.8 Hz, 2H), 2.39 (s, 3H), 2.22 (s, 3H), 2.17−2.10 (m, 1H), 2.04−1.86 (m, 2H), 1.81−1.66 (m, 3H), 1.36 (s, 3H), 1.36 (s, 3H), 1.18 (s, 9H). ^{13}C{^{1}H} NMR (126 MHz, $CDCl_3$): δ 177.2, 156.2, 156.0, 154.1, 143.9, 143.2, 141.9, 134.9, 133.1, 132.9, 129.5, 129.2, 129.1, 128.4, 127.4, 122.7, 122.5, 78.4, 60.3, 51.5, 31.8, 28.9, 28.3, 25.7, 16.6, 15.1, 14.7, 14.6; ^{11}B NMR (128 MHz, $CDCl_3$): δ 1.80 (s). HRMS (ESI-TOF) m/z [M + H]$^+$ calcd for $C_{30}H_{38}BN_6O_4$, 557.3047; found, 557.3050. Compound **8C** was obtained as an orange solid (23.1 mg, 0.028 mmol, 18.0%): ^{1}H NMR (400 MHz, $CDCl_3$): δ 7.51−7.44 (m, 3H), 7.42−7.34 (m, 2H), 5.94 (s, 2H), 5.13 (d, J = 7.6 Hz, 2H), 4.36−4.25 (m, 2H), 3.33−3.19 (m, 4H), 2.39 (s, 6H), 1.95 (bs, 2H), 1.70−1.55 (m, 6H), 1.41 (s, 18H), 1.40 (s, 6H), 1.28 (m, 8.1 Hz, 2H). ^{13}C{^{1}H} NMR (126 MHz, $CDCl_3$): δ 172.3, 155.3, 153.3, 143.4, 134.9, 132.7, 129.0, 129.0, 128.2, 121.5, 79.5, 54.1, 51.4, 32.6, 29.3, 28.4, 22.5, 14.7, 14.6; ^{11}B NMR (128 MHz, $CDCl_3$): δ 0.00 (s). HRMS (ESI-TOF) m/z [M + Na]$^+$ calcd for $C_{41}H_{57}BNaN_{10}O_8$, 851.4359; found, 851.4353.

BODIPY **9** was synthesized using *N*-α-Boc-*N*-ε-benzyloxycarbonyl-L-lysine (234.7 mg, 0.617 mmol) and purified by preparative TLC plates using ethyl acetate/hexanes (1:2) for elution. Compound **9A** (trace, not isolated). Compound **9B** was obtained as an orange solid (37.0 mg, 0.056 mmol, 36.1%): ^{1}H NMR (500 MHz, CD_2Cl_2): δ 7.53−7.46 (m, 3H), 7.36−7.22 (m, 7H), 6.02 (d, J = 3.6 Hz, 2H), 5.12 (s, 1H), 5.06 (s, 2H), 4.07 (d, J = 6.4 Hz, 1H), 3.27−3.18 (m,

https://doi.org/10.1021/acs.joc.1c02328
J. Org. Chem. 2021, 86, 18030−18041

2H), 2.36 (s, 3H), 2.20 (s, 3H), 2.07 (s, 1H), 1.95−1.85 (m, 2H), 1.65−1.57 (m, 3H), 1.38 (s, 3H), 1.37 (s, 3H), 1.16 (s, 9H). $^{13}C\{^1H\}$ NMR (126 MHz, CD_2Cl_2): δ 177.1, 156.3, 156.2, 156.1, 154.3, 144.0, 143.3, 142.0, 137.2, 134.9, 133.1, 132.9, 129.5, 129.1, 128.4, 127.8, 127.8, 127.6, 122.5, 122.5, 78.2, 66.2, 60.3, 40.8, 29.7, 29.4, 28.0, 25.7, 14.9, 14.5, 14.4; ^{11}B NMR (128 MHz, CD_2Cl_2): δ 1.81 (s). HRMS (ESI-TOF) *m/z* $[M + Na]^+$ calcd for $C_{38}H_{45}BNaN_4O_6$, 687.3336; found, 687.3340. Compound **9C** was obtained as an orange solid (48.0 mg, 0.046 mmol, 29.8%): ^1H NMR (400 MHz, $CDCl_3$): δ 7.51−7.44 (m, 3H), 7.41−7.28 (m, 12H), 5.91 (s, 2H), 5.15 (s, 2H), 5.09 (s, 4H), 4.87 (s, 2H), 4.27 (s, 2H), 3.17 (d, *J* = 6.0 Hz, 4H), 2.36 (s, 6H), 1.91 (s, 2H), 1.67 (s, 5H), 1.53 (s, 5H), 1.40 (s, 18H), 1.37 (s, 6H). $^{13}C\{^1H\}$ NMR (126 MHz, $CDCl_3$): δ 172.4, 156.4, 155.4, 153.3, 143.4, 142.7, 136.6, 134.9, 132.7, 129.0, 128.9, 128.5, 128.2, 128.1, 121.5, 79.5, 66.6, 54.0, 40.9, 32.8, 28.4, 22.5, 14.7, 14.6; ^{11}B NMR (128 MHz, $CDCl_3$): δ 0.00 (s). HRMS (ESI-TOF) *m/z* $[M + Na]^+$ calcd for $C_{57}H_{73}BNaN_6O_{12}$, 1067.5281; found, 1067.5288.

BODIPY **10** was synthesized using *N*-Boc-L-glutamine (152.0 mg, 0.616 mmol) and purified by preparative TLC using dichloromethane/methanol/ammonium hydroxide in a 90:9.5:0.5 ratio for elution. Compound **10A** was obtained as an orange solid (7.3 mg, 0.013 mmol, 8.6%). ^1H NMR (400 MHz, $CDCl_3$): δ 7.52−7.45 (m, 3H), 7.40−7.36 (m, 1H), 7.30−7.27 (m, 1H), 6.41 (s, 1H), 5.96 (s, 2H), 5.37−5.28 (m, 1H), 4.27 (d, *J* = 5.6 Hz, 1H), 2.48 (s, 3H), 2.47 (s, 3H), 2.36−2.25 (m, 2H), 1.91−1.80 (m, 1H), 1.41 (s, 9H), 1.39 (s, 6H). $^{13}C\{^1H\}$ NMR (126 MHz, $CDCl_3$): δ 174.7, 171.6, 156.1, 154.8, 154.6, 143.4, 142.4, 134.9, 132.3, 129.2, 129.0, 129.0, 128.1, 127.9, 121.4, 121.3, 79.8, 53.7, 32.2, 30.1, 28.3, 14.7, 14.5; ^{11}B NMR (128 MHz, $CDCl_3$): δ 0.39 (d, *J* = 22.9 Hz). HRMS (ESI-TOF) *m/z* $[M + Na]^+$ calcd for $C_{29}H_{36}BFNaN_4O_5$ 573.2660; found, 573.2675. Compound **10B** was obtained as an orange solid (0.037 mmol, 24.3%). ^1H NMR (500 MHz, $CDCl_3$): δ 7.54−7.43 (m, 3H), 7.25−7.15 (m, 2H), 6.00 (d, *J* = 9.5 Hz, 2H), 4.20 (dd, *J* = 9.4, 2.4 Hz, 1H), 2.85−2.77 (m, 2H), 2.51−2.42 (m, 1H), 2.40 (s, 3H), 2.29−2.24 (m, 1H), 2.22 (s, 3H), 1.38 (s, 3H), 1.37 (s, 3H), 1.19 (s, 9H). $^{13}C\{^1H\}$ NMR (126 MHz, $CDCl_3$): δ 176.7, 174.9, 156.7, 156.1, 154.0, 144.1, 143.3, 141.9, 134.9, 133.1, 133.0, 129.6, 129.2, 129.1, 128.4, 127.4, 122.9, 122.6, 78.9, 59.3, 33.7, 28.2, 27.0, 14.7, 14.6; ^{11}B NMR (128 MHz, CD_3OD): δ 1.87 (s). HRMS (ESI-TOF) *m/z* $[M + Na]^+$ calcd for $C_{29}H_{35}BNaN_4O_5$ 553.2598; found, 553.2607. Compound **10C** was obtained as an orange solid (30.4 mg, 0.039 mmol, 25.4%). ^1H NMR (400 MHz, $CDCl_3$): δ 7.52−7.43 (m, 3H), 7.40−7.32 (m, 2H), 6.69 (bs, 2H), 5.95 (s, 2H), 5.84 (bs, 2H), 5.39 (d, *J* = 7.8 Hz, 2H), 4.25 (bs, 2H), 2.38 (s, 6H), 2.35−2.24 (m, 4H), 1.95−1.79 (m, 2H), 1.40 (s, 18H), 1.36 (s, 6H). $^{13}C\{^1H\}$ NMR (126 MHz, $CDCl_3$): δ 175.1, 171.7, 155.9, 153.5, 143.4, 142.7, 134.8, 132.6, 129.0, 128.9, 128.0, 121.6, 79.8, 69.5, 53.7, 32.3, 28.3, 14.8, 14.6; ^{11}B NMR (128 MHz, $CDCl_3$): δ 0.01 (s). HRMS (ESI-TOF) *m/z* $[M + Na]^+$ calcd for $C_{39}H_{53}BNaN_6O_{10}$ 799.3815; found, 799.3817.

BODIPY **11** was synthesized using *N*-Boc-Gly-Gly-Gly (234.7 mg, 0.617 mmol) and purified by preparative TLC plates using ethyl acetate/hexanes (1:2) for elution. Compound **11A** (trace, not isolated). Compound **11B** was obtained as an orange solid (23.0 mg, 0.040 mmol, 26.0%): ^1H NMR (400 MHz, $CDCl_3$): δ 7.67−7.57 (m, 2H), 7.55−7.47 (m, 2H), 7.32−7.27 (m, 1H), 6.85 (s, 1H), 6.06 (s, 2H), 5.04 (s, 1H), 4.24 (s, 2H), 3.78 (d, *J* = 5.5 Hz, 2H), 3.36 (d, *J* = 3.7 Hz, 2H), 2.27 (s, 6H), 1.44 (s, 9H), 1.42 (s, 6H). $^{13}C\{^1H\}$ NMR (126 MHz, $CDCl_3$): δ 172.6, 168.8, 155.8, 145.6, 143.5, 134.1, 132.7, 130.0, 129.4, 129.1, 128.3, 127.3, 123.5, 80.3, 50.2, 41.1, 29.7, 28.3, 14.8, 14.7; ^{11}B NMR (128 MHz, CDCl3): δ 1.95 (s). HRMS (ESI-TOF) *m/z* $[M + H]^+$ calcd for $C_{30}H_{37}BN_5O_6$, 574.2837; found, 574.2828. Compound **11C** was obtained as an orange solid (26.0 mg, 0.030 mmol, 19.5%):^1H NMR (400 MHz, CDCl3): δ 7.51−7.42 (m, 3H), 7.32 (d, *J* = 7.3 Hz, 2H), 7.25−7.20 (m, 1H), 7.04 (s, 2H), 5.92 (s, 2H), 5.57 (s, 2H), 3.92 (dd, *J* = 16.6, 5.0 Hz, 8H), 3.76 (d, *J* = 3.5 Hz, 4H), 2.50 (s, 2H), 2.34 (s, 6H), 2.15 (s, 1H), 1.39 (s, 18H), 1.36 (s, 6H). $^{13}C\{^1H\}$ NMR (126 MHz, $CDCl_3$): δ 170.3, 169.2, 169.1, 156.3, 153.7, 143.5, 142.8, 134.8, 132.6, 129.2, 129.0, 128.0, 121.6, 80.3, 69.5, 54.0, 44.1, 42.6, 42.4, 31.7, 31.6, 30.9, 29.7, 29.3, 28.3, 22.6, 14.6, 14.5, 14.1; ^{11}B NMR (128 MHz, $CDCl_3$): δ −0.23 (s). HRMS (ESI-TOF) *m/z* $[M + Na]^+$ calcd for $C_{41}H_{55}BNaN_8O_{12}$, 885.3930; found, 885.3935.

Removal of Side Chain-Protecting Groups of α-Amino Acid-BODIPY Derivatives. To a 10 mL reaction flask were added 2 mL of methanol and 10% Pd/C (10 mg). After purging the solution with hydrogen for 10 min, the amino acid−BODIPY compounds **2**−**4**, and **7** (10 mg) in a mixture of dichloromethane/methanol (1/1) (1 mL) were added, and the reaction mixture was stirred until the disappearance of the starting material. When the starting material disappeared, the Pd/C was filtered. The mixture was then concentrated under vacuum, giving the corresponding products in quantitative yields.

BODIPY **2b** was obtained as an orange solid (8.4 mg, 0.016 mmol, 98.9%): ^1H NMR (400 MHz, $CDCl_3$): δ 7.54−7.47 (m, 3H), 7.29−7.27 (m, 1H), 7.25−7.19 (m, 1H), 6.03 (s, 2H), 4.74 (bs, 1H), 3.18−3.07 (m, 2H), 2.32 (s, 3H), 2.28 (s, 3H), 1.40 (s, 3H), 1.38 (s, 3H), 1.21 (s, 9H). $^{13}C\{^1H\}$ NMR (126 MHz, $CDCl_3$): δ 175.5, 155.5, 154.4, 144.2, 143.8, 142.1, 134.7, 133.2, 133.0, 129.6, 129.3, 129.2, 128.3, 127.3, 122.9, 122.8, 80.0, 56.7, 38.6, 28.2, 16.3, 15.2, 14.7; ^{11}B NMR (128 MHz, $CDCl_3$): δ 1.78 (s). HRMS (ESI-TOF) *m/z* $[M + H]^+$ calcd for $C_{28}H_{33}BN_3O_6$, 518.2462; found, 518.2459. Compound **2c** was obtained as an orange solid (7.9 mg, 0.011 mmol, 98.0%): ^1H NMR (500 MHz, $CDCl_3$): δ 7.55−7.44 (m, 3H), 7.36 (d, *J* = 6.1 Hz, 2H), 5.97 (s, 1H), 5.42 (d, *J* = 5.8 Hz, 2H), 4.64 (bs, 2H), 3.26 (d, *J* = 13.3 Hz, 2H), 2.50 (dd, *J* = 14.7, 10.4 Hz, 2H), 2.38 (s, 6H), 1.41 (s, 18H), 1.40 (s, 6H). $^{13}C\{^1H\}$ NMR (126 MHz, $CDCl_3$): δ 176.7, 175.2, 170.4, 155.2, 154.2, 143.7, 142.7, 134.8, 132.6, 129.2, 129.1, 128.0, 121.9, 80.0, 51.7, 38.0, 28.3, 20.5, 14.7, 14.6; ^{11}B NMR (128 MHz, $CDCl_3$): δ 0.01 (s). HRMS (ESI-TOF) *m/z* $[M + Na]^+$ calcd for $C_{37}H_{47}BNaN_4O_{12}$, 773.3182; found, 773.3188.

BODIPY **3b** was obtained as an orange solid (6.1 mg, 0.011 mmol, 90.0%): ^1H NMR (400 MHz, $CDCl_3$): δ 7.50 (s, 3H), 7.39−7.34 (m, 1H), 7.26−7.21 (m, 1H), 6.03 (s, 1H), 6.00 (s, 1H), 4.21−4.13 (m, 1H), 3.44−3.29 (m, 2H), 2.40 (s, 3H), 2.24 (s, 3H), 2.16−1.98 (m, 4H), 1.39 (s, 3H), 1.38 (s, 3H), 1.19 (s, 9H). $^{13}C\{^1H\}$ NMR (126 MHz, $CDCl_3$): δ 177.2, 156.7, 156.5, 153.9, 144.2, 143.1, 141.8, 134.9, 133.0, 129.5, 129.1, 128.4, 127.5, 123.1, 122.6, 79.1, 59.9, 40.8, 29.3, 28.3, 27.5, 16.8, 15.2, 14.8, 14.6; ^{11}B NMR (128 MHz, $CDCl_3$): δ 1.84 (s). HRMS (ESI-TOF) *m/z* $[M + H]^+$ calcd for $C_{30}H_{40}BN_6O_4$, 559.3204; found, 559.3222. Compound **3c** was obtained as an orange solid (6.0 mg, 0.007 mmol, 93%): ^1H NMR (400 MHz, CD_3OD): δ 7.59−7.51 (m, 3H), 7.44−7.39 (m, 2H), 6.00 (s, 2H), 4.12 (bs, 2H), 3.24−3.16 (m, 4H), 2.46 (s, 6H), 1.90 (bs, *J* = 8.0 Hz, 2H), 1.72−1.59 (m, 8H), 1.44 (s, 18H), 1.39 (s, 6H). $^{13}C\{^1H\}$ NMR (126 MHz, CD_3OD): δ 172.8, 157.2, 156.7, 153.6, 143.1, 135.2, 132.7, 128.9, 128.8, 128.0, 120.8, 79.2, 69.2, 54.7, 54.3, 40.6, 30.7, 28.6, 28.1, 27.4, 25.2, 13.9, 13.2; ^{11}B NMR (128 MHz, CD_3OD): δ 0.08 (s). HRMS (ESI-TOF) *m/z* $[M + H]^+$ calcd for $C_{41}H_{62}BN_{10}O_8$, 833.4847; found, 833.4842.

BODIPY **4b** was obtained as an orange solid (7.7 mg, 0.014 mmol, 96.1%): ^1H NMR (400 MHz, $CDCl_3$): δ 7.73 (s, 1H), 7.54−7.45 (m, 3H), 7.30−7.27 (m, 1H), 7.23 (bs, 1H), 7.05 (s, 1H), 6.02 (d, *J* = 13.6 Hz, 2H), 4.81 (bs, 1H), 4.36 (d, *J* = 6.4 Hz, 1H), 3.54−3.43 (m, 1H), 3.36−3.25 (m, 1H), 2.42 (s, 3H), 2.18 (s, 3H), 1.39 (s, 6H), 1.22 (s, 9H). $^{13}C\{^1H\}$ NMR (126 MHz, $CDCl_3$): δ 177.6, 156.5, 155.7, 154.2, 144.3, 143.7, 142.1, 134.8, 133.0, 129.6, 129.3, 129.2, 129.0, 128.3, 127.4, 124.6, 122.9, 122.7, 79.3, 60.8, 28.3, 27.9, 16.5, 15.2, 14.7; ^{11}B NMR (128 MHz, $CDCl_3$): δ 1.92 (s). HRMS (ESI-TOF) *m/z* $[M + H]^+$ calcd for $C_{30}H_{35}BN_5O_4$ 540.2782; found, 540.2795. Compound **4c** was obtained as an orange solid (7.3 mg, 0.009 mmol, 97.3%): ^1H NMR (400 MHz, $CDCl_3$): δ 7.81 (s, 2H), 7.50−7.43 (m, 3H), 7.37−7.33 (m, 2H), 6.89 (s, 2H), 5.91 (s, 2H), 5.43 (d, *J* = 7.1 Hz, 2H), 5.11 (bs, 4H), 4.50 (bs, 2H), 3.26 (dd, *J* = 14.7, 4.5 Hz, 2H), 2.97 (dd, *J* = 13.9, 6.3 Hz, 2H), 2.18 (s, 6H), 1.38 (s, 6H), 1.35 (s, 18H). $^{13}C\{^1H\}$ NMR (126 MHz, $CDCl_3$): δ 171.6, 155.4, 143.4, 134.9, 134.6, 132.6, 129.1, 129.0, 128.1, 121.6, 79.7, 54.4, 30.3, 29.3, 28.3, 14.6, 14.5; ^{11}B NMR (128 MHz, $CDCl_3$): δ 0.02 (s). HRMS (ESI-TOF) *m/z* $[M + H]^+$ calcd for $C_{41}H_{52}BN_8O_8$ 795.4003; found, 795.3995.

https://doi.org/10.1021/acs.joc.1c02328
J. Org. Chem. 2021, 86, 18030−18041

BODIPY **7b** was obtained as an orange solid (8.1 mg, 0.016 mmol, 95.5%): ^{1}H NMR (500 MHz, CD_2Cl_2): δ 7.61−7.45 (m, 3H), 7.34−7.18 (m, 2H), 6.06 (s, 2H), 5.01 (s, 1H), 4.54−4.39 (m, 1H), 4.25−4.01 (m, 2H), 2.29 (s, 3H), 2.27 (s, 3H), 1.41 (s, 6H), 1.21 (s, 9H). ^{13}C{^{1}H} NMR (126 MHz, CD_2Cl_2): δ 173.7, 158.2, 155.9, 154.5, 144.3, 143.8, 142.3, 134.8, 133.3, 133.1, 129.6, 129.3, 129.2, 128.5, 127.6, 122.8, 122.7, 100.1, 79.6, 64.7, 64.5, 28.1, 16.3, 15.2, 14.5; ^{11}B NMR (128 MHz, CD_2Cl_2): δ 1.64 (s). HRMS (ESI-TOF) m/z [M + H]$^+$ calcd for $C_{27}H_{33}BN_3O_5$, 490.2513; found, 490.2532. Compound **7c** was obtained as an orange solid (8.2 mg, 0.011 mmol, 94%): ^{1}H NMR (400 MHz, $CDCl_3$): δ 7.48 (m, 3H), 7.40−7.31 (m, 2H), 5.95 (s, 2H), 5.50 (d, J = 5.5 Hz, 2H), 4.32 (bs, 2H), 4.02 (bs, 4H), 2.42 (s, 6H), 1.42 (s, 9H), 1.40 (s, 6H). ^{13}C{^{1}H} NMR (126 MHz, $CDCl_3$): δ 170.3, 155.9, 153.9, 143.4, 142.6, 134.9, 132.6, 129.1, 129.0, 128.1, 121.7, 80.0, 63.9, 56.8, 28.3, 14.6, 14.5; ^{11}B NMR (128 MHz, $CDCl_3$): δ 0.08 (s). HRMS (ESI-TOF) m/z [M + H]$^+$ calcd for $C_{35}H_{47}BNaN_4O_{10}$, 717.3284; found, 717.3317.

■ ASSOCIATED CONTENT

Supporting Information

The Supporting Information is available free of charge at https://pubs.acs.org/doi/10.1021/acs.joc.1c02328.

^{1}H, ^{13}C, and ^{11}B NMR spectra, cytotoxicity, fluorescence imaging, and frontier orbitals of BODIPYs (PDF)

■ AUTHOR INFORMATION

Corresponding Author

M. Graça H. Vicente − *Department of Chemistry, Louisiana State University, Baton Rouge, Louisiana 70803, United States;* orcid.org/0000-0002-4429-7868; Email: vicente@lsu.edu

Authors

Maodie Wang − *Department of Chemistry, Louisiana State University, Baton Rouge, Louisiana 70803, United States*

Guanyu Zhang − *Department of Chemistry, Louisiana State University, Baton Rouge, Louisiana 70803, United States;* orcid.org/0000-0002-3202-2939

Petia Bobadova-Parvanova − *Department of Chemistry and Fermentation Sciences, Appalachian State University, Boone, North Carolina 28607, United States;* orcid.org/0000-0002-1965-419X

Kevin M. Smith − *Department of Chemistry, Louisiana State University, Baton Rouge, Louisiana 70803, United States;* orcid.org/0000-0002-6736-4779

Complete contact information is available at: https://pubs.acs.org/10.1021/acs.joc.1c02328

Author Contributions

[§]M.W. and G.Z. contributed equally.

Funding

This work was supported by the National Science Foundation, grant CHE-1800126.

Notes

The authors declare no competing financial interest.

■ ACKNOWLEDGMENTS

This work was supported by the National Science Foundation (CHE-1362641). The authors are thankful to the Louisiana Optical Network Initiative (www.loni.org) for the use of their computer facilities. P.B.-P. is grateful to Rockhurst University, Kansas City, MO 64110, United States, for the support during the initial stages of this research.

■ REFERENCES

(1) Loudet, A.; Burgess, K. BODIPY Dyes and Their Derivatives: Syntheses and Spectroscopic Properties. *Chem. Rev.* **2007**, *107*, 4891−4932.

(2) Ziessel, R.; Ulrich, G.; Harriman, A. The Chemistry of Bodipy: A new El Dorado for Fluorescence Tools. *New J. Chem.* **2007**, *31*, 496−499.

(3) Ulrich, G.; Ziessel, R.; Harriman, A. The Chemistry of Fluorescent Bodipy Dyes: Versatility Unsurpassed. *Angew. Chem., Int. Ed. Engl.* **2008**, *47*, 1184−1201.

(4) Kamkaew, A.; Lim, S. H.; Lee, H. B.; Kiew, L. V.; Chung, L. Y.; Burgess, K. BODIPY dyes in photodynamic therapy. *Chem. Soc. Rev.* **2013**, *42*, 77−88.

(5) Lu, H.; Mack, J.; Yang, Y.; Shen, Z. Structural modification strategies for the rational design of red/NIR region BODIPYs. *Chem. Soc. Rev.* **2014**, *43*, 4778−4823.

(6) Boens, N.; Verbelen, B.; Ortiz, M. J.; Jiao, L.; Dehaen, W. Synthesis of BODIPY dyes through postfunctionalization of the boron dipyrromethene core. *Coord. Chem. Rev.* **2019**, *399*, 213024.

(7) Kolemen, S.; Akkaya, E. U. Reaction-Based BODIPY Probes for Selective Bio-Imaging. *Coord. Chem. Rev.* **2017**, *354*, 121−134.

(8) Wu, Q.; Jia, G.; Tang, B.; Guo, X.; Wu, H.; Yu, C.; Hao, E.; Jiao, L. Conformationally Restricted α, α Directly Linked BisBODIPYs as Highly Fluorescent Near-Infrared Absorbing Dyes. *Org. Lett.* **2020**, *22*, 9239−9243.

(9) Kamkaew, A.; Lim, S. H.; Lee, H. B.; Kiew, L. V.; Chung, L. Y.; Burgess, K. BODIPY Dyes in Photodynamic Therapy. *Chem. Soc. Rev.* **2013**, *42*, 77−88.

(10) Wang, J.; Gong, Q.; Wang, L.; Hao, E.; Jiao, L. The main strategies for tuning BODIPY fluorophores into photosensitizers. *J. Porphyrins Phthalocyanines* **2020**, *24*, 603−635.

(11) Boens, N.; Leen, V.; Dehaen, W. Fluorescent Indicators Based on BODIPY. *Chem. Soc. Rev.* **2012**, *41*, 1130−1172.

(12) Bessette, A.; Hanan, G. S. Design, Synthesis and Photophysical Studies of Dipyrromethene-Based Materials: Insights into Their Applications in Organic Photovoltaic Devices. *Chem. Soc. Rev.* **2014**, *43*, 3342−3405.

(13) Miao, W.; Yu, C.; Hao, E.; Jiao, L. Functionalized BODIPYs as Fluorescent Molecular Rotors for Viscosity Detection. *Front. Chem.* **2019**, *7*, 825.

(14) Boens, N.; Verbelen, B.; Dehaen, W. Postfunctionalization of the BODIPY core: synthesis and spectroscopy. *Eur. J. Org. Chem.* **2015**, *2015*, 6577−6595.

(15) Bañuelos, J.; Martín, V.; Gómez-Durán, C. F. A.; Córdoba, I. J. A.; Peña-Cabrera, E.; García-Moreno, I.; Costela, Á.; Pérez-Ojeda, M. E.; Arbeloa, T.; Arbeloa, Í. L. New 8-Amino-BODIPY derivatives: Surpassing laser dyes at blue-edge wavelengths. *Chem.—Eur. J.* **2011**, *17*, 7261−7270.

(16) Gómez-Durán, C. F. A.; García-Moreno, I.; Costela, A.; Martin, V.; Sastre, R.; Bañuelos, J.; López Arbeloa, F.; López Arbeloa, I.; Peña-Cabrera, E. 8-PropargylaminoBODIPY: unprecedented blue-emitting pyrromethene dye. Synthesis, photophysics and laser properties. *Chem. Commun.* **2010**, *46*, 5103−5105.

(17) Jagtap, K. K.; Shivran, N.; Mula, S.; Naik, D. B.; Sarkar, S. K.; Mukherjee, T.; Maity, D. K.; Ray, A. K. Change of boron substitution improves the lasing performance of BODIPY dyes: a mechanistic rationalisation. *Chem.—Eur. J.* **2013**, *19*, 702−708.

(18) Yang, L.; Simionescu, R.; Lough, A.; Yan, H. Some Observations Relating to The Stability of the BODIPY Fluorophore under Acidic and Basic Conditions. *Dyes Pigm.* **2011**, *91*, 264−267.

(19) Nguyen, A. L.; Wang, M.; Bobadova-Parvanova, P.; Do, Q.; Zhou, Z.; Fronczek, F. R.; Smith, K. M.; Vicente, M. G. H. Synthesis and properties of B-cyano-BODIPYs. *J. Porphyrins Phthalocyanines* **2016**, *20*, 1409−1419.

(20) Wang, M.; Vicente, M. G. H.; Mason, D.; Bobadova-Parvanova, P. Stability of a Series of BODIPYs in Acidic Conditions: An Experimental and Computational Study into the Role of the Substituents at Boron. *ACS Omega* **2018**, *3*, 5502−5510.

(21) Klenner, M. A.; Pascali, G.; Massi, M.; Fraser, B. H. Fluorine-18 Radiolabelling and Photophysical Characteristics of Multimodal PET−Fluorescence Molecular Probes. *Chem.—Eur. J.* **2021**, *27*, 861−876.
(22) Ziessel, R.; Goze, C.; Ulrich, G. Design and Synthesis of Alkyne-Substituted Boron in Dipyrromethene Frameworks. *Synthesis* **2007**, *2007*, 936−949.
(23) Zhang, G.; Wang, M.; Fronczek, F. R.; Smith, K. M.; Vicente, M. G. H. Lewis-acid-catalyzed BODIPY boron functionalization using trimethylsilyl nucleophiles. *Inorg. Chem.* **2018**, *57*, 14493−14496.
(24) Ray, C.; Díaz-Casado, L.; Avellanal-Zaballa, E.; Bañuelos, J.; Cerdán, L.; García-Moreno, I.; Moreno, F.; Maroto, B. L.; López-Arbeloa, Í.; de la Moya, S. N -BODIPYs Come into Play: Smart Dyes for Photonic Materials. *Chem.—Eur. J.* **2017**, *23*, 9383−9390.
(25) Bodio, E.; Goze, C. Investigation of B-F substitution on BODIPY and aza-BODIPY dyes: Development of B-O and B-C BODIPYs. *Dyes Pigm.* **2019**, *160*, 700−710.
(26) Sánchez-Carnerero, E. M.; Gartzia-Rivero, L.; Moreno, F.; Maroto, B. L.; Agarrabeitia, A. R.; Ortiz, M. J.; Bañuelos, J.; López-Arbeloa, Í.; de la Moya, S. Spiranic BODIPYs: a ground-breaking design to improve the energy transfer in molecular cassettes. *Chem. Commun.* **2014**, *50*, 12765−12767.
(27) Manzano, H.; Esnal, I.; Marqués-Matesanz, T.; Bañuelos, J.; López-Arbeloa, I.; Ortiz, M. J.; Cerdán, L.; Costela, A.; García-Moreno, I.; Chiara, J. L. Unprecedented J-Aggregated Dyes in Pure Organic Solvents. *Adv. Funct. Mater.* **2016**, *26*, 2756−2769.
(28) Yuan, K.; Wang, X.; Mellerup, S. K.; Kozin, I.; Wang, S. Spiro-BODIPYs with a Diaryl Chelate: Impact on Aggregation and Luminescence. *J. Org. Chem.* **2017**, *82*, 13481−13487.
(29) Mendive-Tapia, L.; Zhao, C.; Akram, A. R.; Preciado, S.; Albericio, F.; Lee, M.; Serrels, A.; Kielland, N.; Read, N. D.; Lavilla, R.; Vendrell, M. Spacer-free BODIPY fluorogens in antimicrobial peptides for direct imaging of fungal infection in human tissue. *Nat. Commun.* **2016**, *7*, 10940.
(30) Mendive-Tapia, L.; Subiros-Funosas, R.; Zhao, C.; Albericio, F.; Read, N. D.; Lavilla, R.; Vendrell, M. Preparation of a Trp-BODIPY fluorogenic amino acid to label peptides for enhanced live-cell fluorescence imaging. *Nat. Protoc.* **2017**, *12*, 1588−1619.
(31) Farinone, M.; Cybińska, J.; Pawlicki, M. BODIPY-amino acid conjugates−tuning the optical response with a meso-heteroatom. *Org. Chem. Front.* **2020**, *7*, 2391−2398.
(32) Wang, M.; Zhang, G.; Bobadova-Parvanova, P.; Merriweather, A. N.; Odom, L.; Barbosa, D.; Fronczek, F. R.; Smith, K. M.; Vicente, M. G. H. Synthesis and Investigation of Linker-Free BODIPY−Gly Conjugates Substituted at the Boron Atom. *Inorg. Chem.* **2019**, *58*, 11614−11621.
(33) Wang, M.; Zhang, G.; Kaufman, N. E. M.; Bobadova-Parvanova, P.; Fronczek, F. R.; Smith, K. M.; Vicente, M. G. H. Linker-Free Near-IR Aza-BODIPY-Glutamine Conjugates Through Boron Functionalization. *Eur. J. Org. Chem.* **2020**, *2020*, 971−977.
(34) Smoum, R.; Rubinstein, A.; Dembitsky, V. M.; Srebnik, M. Boron Containing Compounds as Protease Inhibitors. *Chem. Rev.* **2012**, *112*, 4156−4220.
(35) Adamczyk-Woźniak, A.; Borys, K. M.; Sporzynski, A. Recent developments in the chemistry and biological applications of benzoxaboroles. *Chem. Rev.* **2015**, *115*, 5224−5247.
(36) Yang, F.; Zhu, M.; Zhang, J.; Zhou, H. Synthesis of biologically active boron-containing compounds. *MedChemComm* **2018**, *9*, 201−211.
(37) Fernandes, G. F. S.; Denny, W. A.; Dos Santos, J. L. Boron in drug design: Recent advances in the development of new therapeutic agents. *Eur. J. Med. Chem.* **2019**, *179*, 791−804.
(38) Yinghuai, Z.; Lin, X.; Xie, H.; Li, J.; Hosmane, N. S.; Zhang, Y. The Current Status and Perspectives of Delivery Strategy for Boronbased Drugs. *Curr. Med. Chem.* **2019**, *26*, 5019−5035.
(39) Baldwin, A. G.; Rivers-Auty, J.; Daniels, M. J. D.; White, C. S.; Schwalbe, C. H.; Schilling, T.; Hammadi, H.; Jaiyong, P.; Spencer, N. G.; England, H.; Luheshi, N. M.; Kadirvel, M.; Lawrence, C. B.; Rothwell, N. J.; Harte, M. K.; Bryce, R. A.; Allan, S. M.; Eder, C.; Freeman, S.; Brough, D. Boron-Based Inhibitors of the NLRP3 Inflammasome. *Cell Chem. Biol.* **2017**, *24*, 1321−1335.
(40) Baldwin, A. G.; Tapia, V. S.; Swanton, T.; White, C. S.; Beswick, J. A.; Brough, D.; Freeman, S. Design, Synthesis and Evaluation of Oxazaborine Inhibitors of the NLRP3 Inflammasome. *ChemMedChem* **2018**, *13*, 312−320.
(41) Nguyen, A. L.; Bobadova-Parvanova, P.; Hopfinger, M.; Fronczek, F. R.; Smith, K. M.; Vicente, M. G. H. Synthesis and reactivity of 4, 4-dialkoxy-BODIPYs: an experimental and computational study. *Inorg. Chem.* **2015**, *54*, 3228−3236.
(42) Isidro-Llobet, A.; Álvarez, M.; Albericio, F. Amino Acid-Protecting Groups. *Chem. Rev.* **2009**, *109*, 2455−2504.
(43) Groves, B. R.; Crawford, S. M.; Lundrigan, T.; Matta, C. F.; Sowlati-Hashjin, S.; Thompson, A. Synthesis and characterisation of the unsubstituted dipyrrin and 4, 4-dichloro-4-bora-3a, 4a-diaza-s-indacene: improved synthesis and functionalisation of the simplest BODIPY framework. *Chem. Commun.* **2013**, *49*, 816−818.
(44) Lundrigan, T.; Crawford, S. M.; Cameron, T. S.; Thompson, A. Cl-BODIPYs: a BODIPY class enabling facile B-substitution. *Chem. Commun.* **2012**, *48*, 1003−1005.
(45) Diaz-Rodriguez, R. M.; Burke, L.; Robertson, K. N.; Thompson, A. Synthesis, properties and reactivity of BCl 2 aza-BODIPY complexes and salts of the aza-dipyrrinato scaffold. *Org. Biomol. Chem.* **2020**, *18*, 2139−2147.
(46) Crawford, S. M.; Thompson, A. Conversion of 4, 4-Difluoro-4-bora-3a, 4a-diaza-s-indacenes (F-BODIPYs) to Dipyrrins with a Microwave-Promoted Deprotection Strategy. *Org. Lett.* **2010**, *12*, 1424−1427.
(47) Tu, Z.; Volk, M.; Shah, K.; Clerkin, K.; Liang, J. F. Constructing bioactive peptides with pH-dependent activities. *Peptides* **2009**, *30*, 1523−1528.
(48) Sibrian-Vazquez, M.; Jensen, T. J.; Fronczek, F. R.; Hammer, R. P.; Vicente, M. G. H. Synthesis and characterization of positively charged porphyrin− peptide conjugates. *Bioconj. Chem.* **2005**, *16*, 852−863.
(49) Jensen, T. J.; Vicente, M. G. H.; Luguya, R.; Norton, J.; Fronczek, F. R.; Smith, K. M. Effect of overall charge and charge distribution on cellular uptake, distribution and phototoxicity of cationic porphyrins in HEp2 cells. *J. Photochem. Photobiol. B: Biol.* **2010**, *100*, 100−111.
(50) Ditchfield, R.; Hehre, W. J.; Pople, J. A. Self-Consistent Molecular-Orbital Methods. IX. An Extended Gaussian-Type Basis for Molecular-Orbital Studies of Organic Molecules. *J. Chem. Phys.* **1971**, *54*, 724−728.
(51) Lee, C.; Yang, W.; Parr, R. G. Development of the Colle-Salvetti Correlation-Energy Formula into a Functional of the Electron Density. *Phys. Rev. B: Condens. Matter Mater. Phys.* **1988**, *37*, 785.
(52) Becke, A. Gaussian Basis Sets for Use in Correlated Molecular Calculations. III. The Atoms Aluminum through Argon. *J. Chem. Phys.* **1993**, *98*, 1358.
(53) Miertuš, S.; Scrocco, E.; Tomasi, J. Electrostatic Interaction of a Solute with a Continuum. A Direct Utilizaion of AB Initio Molecular Potentials for the Prevision of Solvent Effects. *Chem. Phys.* **1981**, *55*, 117−129.
(54) Tomasi, J.; Mennucci, B.; Cammi, R. Quantum Mechanical Continuum Solvation Models. *Chem. Rev.* **2005**, *105*, 2999−3094.
(55) Bauernschmitt, R.; Ahlrichs, R. Treatment of Electronic Excitations within the Adiabatic Approximation of Time Dependent Density Functional Theory. *Chem. Phys. Lett.* **1996**, *256*, 454−464.
(56) Frisch, M. J.; Trucks, G. W.; Schlegel, H. B.; Scuseria, G. E.; Robb, M. A.; Cheeseman, J. R.; Scalmani, G.; Barone, V.; Mennucci, B.; Petersson, G. A.; Nakatsuji, H.; Caricato, M.; Li, X.; Hratchian, H. P.; Izmaylov, A. F.; Bloino, J.; Zheng, J.; Sonnenberg, J. L.; Hada, M.; Ehara, J.; Toyota, K.; Fukuda, R.; Hasegawa, J.; Ishida, M.; Nakajima, T.; Honda, Y.; Kitao, O.; Nakai, H.; Vreven, T.; Montgomery, J. A., Jr.; Peralta, J. E.; Ogliaro, F.; Bearpark, M.; Heyd, J. J.; Brothers, E.; Kudin, K. N.; Staroverov, V. N.; Keith, T.; Kobayashi, R.; Normand, J.; Raghavachari, K.; Rendell, A.; Burant, J. C.; Iyengar, S. S.; Tomasi, J.; Cossi, M.; Rega, N.; Millam, J. M.; Klene, M.; Knox, J. E.; Cross, J.

https://doi.org/10.1021/acs.joc.1c02328
J. Org. Chem. 2021, 86, 18030−18041

B.; Bakken, V.; Adamo, C.; Jaramillo, J.; Gomperts, R.; Stratmann, R. E.; Yazyev, O.; Austin, A. J.; Cammi, R.; Pomelli, R.; Ochterski, J. W.; Martin, R. L.; Morokuma, K.; Zakrzewski, V. G.; Voth, G. A.; Salvador, P.; Dannenberg, J. J.; Dapprich, S.; Daniels, A. D.; Farkas, O.; Foresman, J. B.; Ortiz, J. V.; Cioslowski, J.; Fox, D. J. *Gaussian 09*, Revision D.01; Gaussian, Inc.: Wallingford CT, 2013.

https://doi.org/10.1021/acs.joc.1c02328
J. Org. Chem. 2021, 86, 18030−18041